INELASTIC BUCKLING TESTS OF RING-STIFFENED CYLINDERS UNDER HYDROSTATIC PRESSURE

by

Lance Boichot
and
Thomas E. Reynolds

May 1965

Report 1992
S-F013 03 02
Task 1951

INELASTIC BUCKLING TESTS OF RING-STIFFENED CYLINDERS UNDER HYDROSTATIC PRESSURE

by

Lance Boichot

and

Thomas E. Reynolds

May 1965

Report 1992
S-F013 03 02
Task 1951

TABLE OF CONTENTS

LIST OF FIGURES

LIST OF TABLES

ABSTRACT

A series of small machined aluminum models were collapsed under external hydrostatic pressure to study the inelastic buckling of near-perfect ring-stiffened cylinders made of strain-hardening materials. The predominant modes of failure were general instability and axisymmetric shell buckling.

Comparisons of test results with the analyses of Lunchick, Krenzke, and Kiernan show promising correlation but additional data would be needed for a complete evaluation.

High bending stresses near frames did not noticeably affect axisymmetric shell buckling strength. The presence of frame fillets, however, caused a significant increase in general instability strength although bending stresses in the absence of fillets were relatively low.

ADMINISTRATIVE INFORMATION

The work was sponsored by the Bureau of Ships under Subproject S-F013 03 02, Task 1951.

INTRODUCTION

Recent efforts in the development of oceanographic vehicles for operation at great depths have led to the consideration of strain-hardening materials such as aluminum and titanium alloys for the pressure hull. Although new structural configurations are also being considered, it is expected that the conventional ring-stiffened cylinder will still find extensive use as the major structural element in many future deep-diving vessels. Methods are therefore needed whereby the collapse depths of stiffened cylindrical hulls made from strain-hardening materials can be accurately determined.

One form of collapse that can occur under hydrostatic pressure is inelastic buckling of the shell between stiffeners in the axisymmetric (spool-shaped) mode. Lunchick[1] has obtained a solution for this case that takes the effects of strain hardening into account, but so far there have been insufficient experimental data for an adequate evaluation of his solution. The objective of the present studies was to provide the necessary data through tests of small machined models with near-perfect circularity having systematic variations in shell thickness, frame spacing, and frame size – the parameters on which shell collapse strength was expected to be critically dependent. It was believed that many small models mass produced at low unit cost and tested with no instrumentation would bring a greater return than would a few expensive, elaborately instrumented models. In this way a wide parametric range could be

[1] References are listed on page 31.

studied at moderate cost. The models were designed to allow some overlap into the range where nonsymmetric buckling (circumferential lobing) of the shell between stiffeners takes place. The transition to this mode is reached as the frame spacing is increased or as the shell thickness is reduced.

As the tests proceeded, however, it became evident that with the range of parameters selected, failures could not be confined to the symmetric mode of shell collapse because of the intervention of a third mode of failure. More often than not, the cylinders were found to fail by inelastic general instability (nonsymmetric buckling of frames and shell together), a mode which had not been believed critical because of the relatively short lengths of the cylinders in question. That this had not been foreseen was due largely to the fact that no method was then available for estimating inelastic general instability strength. Since then an analysis of the problem by Lunchick[2] and a semi-empirical method by Krenzke and Kiernan[3] have been developed. Consequently the present series of tests is also used to evaluate these latter methods. It should be realized, however, that because of the parameters selected for study, those critically affecting general instability strength have received incomplete coverage. The effects, for example, of frame shape and cylinder length have not been adequately explored.

The tests were conducted with 69 small machined aluminum cylinders. In this report the collapse data are presented, comparisons with appropriate theory are made, and conclusions are drawn.

DESCRIPTION OF MODELS

Sixty-nine 2-in.-diameter ring-stiffened cylinders were machined from 7075-T6 aluminum alloy bar stock with a nominal yield strength of 80,000 psi. Each model had six external frames. Although internal frames are normally used in hydrospace vehicle hull design, external frames were chosen for this series of tests because of economy and ease of machining. Furthermore, it was expected that local shell buckling strength would be sensitive to the size of frames but not to their shape; hence all frames were rectangular in cross section.

The models were designed to produce a systematic variation in the nondimensional parameters θ, h/R, and A_f/hL_f

where

$$\theta = \frac{\sqrt[4]{3(1-\nu^2)}\,L}{\sqrt{Rh}}$$

ν is Poisson's ratio,

A_f is the cross-sectional area of the stiffener,

h is the shell thickness,

R is the radius to the midsurface of the shell,

L_f is the distance between frame centers, and

L is the unsupported shell length between stiffeners.

The ranges chosen (1.0-2.5 for θ, 0.02-0.08 for h/R, and 0.2-0.8 for A_f/hL_f) covers the practical geometries for underwater vehicles of strain-hardening materials.

The measured model dimensions together with the yield strength of the material, as determined by the 0.2 percent offset method, are presented in Table 1.

For identification of nominal parameters, the first two digits of the model number represent θ, the third digit represents h/R, and the fourth digit represents A_f/hL_f. Thus, for Model 15-26, θ is 1.5, h/R is 0.02, and A_f/hL_f is 0.6. Compression specimens were taken along the length of bar stock from which the models were machined. A typical compressive stress-strain curve of the aluminum alloy used is shown in Figure 1. Ratios of E_t/E, E_s/E, and $\sqrt{E_s E_t}/E$ (where E is Young's modulus, E_t is the tangent modulus, and E_s is the secant modulus) were determined from these stress-strain curves for various stress levels. Typical plots of these ratios are also shown in Figure 1. These quantities are used in calculating inelastic buckling pressures. A value of 10.8×10^6 psi for Young's modulus was determined by optical measurements; 0.3 was assumed for Poisson's ratio.

An effort was made to minimize the detrimental effects of end conditions by decreasing the length of the two end frame spacings. The spacing of the first frame from each end was 0.8 the spacing (L_f) of the central frames, and the spacing between the first and second frames was 0.9 L_f. To assess the influence of stress concentration on collapse pressure, 22 of the models were duplicated geometries except for the addition of a 1/32-in. fillet radius at the bulkhead-shell intersection and a 1/64-in. fillet radius at the frame-shell intersections. These models are designated by the letter F following the model number.

TEST PROCEDURE AND RESULTS

Each model was tested to collapse under hydrostatic pressure in a 5-in.-diameter tank. Oil was used as a pressure medium. The models were filled with oil and vented to the atmosphere to absorb the energy released at collapse. Pressure was applied in increments, each being held for at least 1 minute. The last increment was normally less than 2 percent of the collapse pressure. Some models collapsed as pressure was applied while others failed under a constant load.

Table 2 gives the observed experimental collapse pressures, the adjusted collapse pressure (which takes into account the additional load due to the external position of the frames), and the mode of failure of the models. The adjusted collapse pressure is the equivalent pressure on a cylinder of constant radius equal to the outer radius of the model

considered.* Figure 2 is a graphical presentation of the adjusted collapse pressure versus the parameter θ and contours of h/R and A_f/hL_f. In determining the values of θ for those models with fillets, the standard submarine design practice was used whereby the faying width of frame is taken to include two-thirds of the fillet width on each side of the frame. This reduced the nominal values of θ as follows: from 2.5 to 2.3, from 2.0 to 1.8, from 1.5 to 1.3, and from 1.0 to 0.8.

Photographs of the collapsed models are shown in Figure 3. It can be seen that extensive damage occurred and that in many cases the shell and frames were torn apart. Figures 3d-3i show that the presence of fillets markedly reduced the extent of this tearing. Models in the upper and lower groups of these figures have identical dimensions, but those in the lower groups have fillets. It was observed (Table 2) that the models with fillets generally had slightly higher collapse strengths than the corresponding models without fillets.

The great majority of models collapsed in the general instability mode. Of the remainder, all except one appeared to have failed in the axisymmetric shell mode. The exception (Model 25-24F) apparently collapsed in the nonsymmetric shell mode. In this respect, the design of the models was successful since some degree of overlap into this mode had been desired. In some cases, particularly those models without fillets, the exact mode of collapse was difficult to distinguish because of extensive destruction; in others, the determination was complicated by the appearance of more than one mode.

Table 3 gives a breakdown of the models in terms of their geometric parameters and modes of collapse. In three cases (25-22F, 20-22F, and 15-22F), calculations showed that stresses at collapse were well within the elastic limit of the material, indicating that collapse occurred by elastic general instability. It was noted that in these three cases, the frames deformed within their planes of curvature whereas for those failing by inelastic general instability, the frames twisted or folded out of their planes (compare, for example, 15-22F with 15-26F or 10-54F).

Referring to Table 3, we see that all models having a nominal θ of 1.0 collapsed by general instability. Models 10-22 and 10-22F also showed axisymmetric deformations. Of the models having a nominal θ of 1.5, those with A_f/L_{fh} less than 0.8 collapsed by general instability. Models with $\theta = 2.5$ and A_f/L_{fh} less than 0.6 likewise failed in that mode with the exception of 25-24F. Local shell failures occurred in all cases where $A_f/L_{fh} = 0.8$ and θ was greater than 1.0 and in those for which $A_f/L_{fh} = 0.6$ and $\theta \geq 2.0$. All shell failures were purely axisymmetric except for Model 25-24F and two others (25-28 and 25-26) where small nonsymmetric deformations were also observed. Figure 3f is a good illustration of the changes in the mode of collapse that can result from progressive increases in frame size.

*In most of the theoretical analyses pertinent to this investigation, the pressure is taken to act at the middle surface of the shell. Thus the additional load acting on all material external to this surface is ignored. Where large external frames or relatively thick shells are concerned (as in some of the geometries considered here), this difference can be significant. Rather than correct each of the computations to give a reduced theoretical pressure, it was found far more convenient and no less accurate to adjust each observed collapse pressure upward in accordance with the load conditions to a pressure comparable to the original computed values.

EVALUATION OF INELASTIC BUCKLING ANALYSES

Since two predominant modes of failure were observed in these tests, it is convenient to group them accordingly before evaluating the various applicable collapse formulas.

Table 4 lists those models which collapsed by general instability together with the ratios of theoretical pressures to the adjusted experimental pressures. The second column lists the ratios for the Lunchick inelastic general instability analysis (Reference 2). The next two columns give the results obtained using two semi-empirical formulas proposed by Krenzke and Kiernan[3] which, for these models, give almost identical results. These are p_t (Equation [1] of Reference 3) and p_{st} (Equation [9] of Reference 3). Also listed in the table is p_a, the pressure at which the average circumferential stress in the frame-shell combination reaches the 0.2 percent offset yield stress of the material. Although not strictly applicable to strain-hardening materials, this pressure is included to illustrate the critical nature of the frame stress in the plastic general instability mode.

In general, these theoretical pressures are somewhat higher than the experimental pressures, most coming within 15 percent. Moreover, there is little to choose between the various formulas, at least for these models, since all theoretical pressures are in close agreement for each case. As was expected for short models such as these (see Reference 3), pressures given by p_t are slightly lower than those given by p_{st}. However, the differences even for the shortest models are at most about 3 percent. Lunchick's pressures are consistently higher than p_{st} but differ only by about the same percentage. It is noted that the models with fillets generally had higher collapse pressures than the others, and in nearly every case, the pressure is in excellent agreement with the calculations.

Perhaps a better way to examine differences between calculations and experiments is through the use of a stability ratio diagram wherein trends may be more easily identified. Figure 1 is such a diagram in which the abscissa is p_{st}/p_e, where p_e is the elastic general instability pressure computed by a modified version of the Bryant formula.[3] Here p_{st} is used as representative of the three inelastic buckling formulas cited. The ordinate is p_c/p_e, p_c being the adjusted experimental collapse pressure. One can immediately see that for cases having high margins of stability (i.e., where p_{st}/p_e is small), the agreement between theory and experiment is quite good. But for the less stable shells (larger values of p_{st}/p_e), note that the experimental points tend to fall below the line ($p_{st} = p_c$) although the agreement is still good for the models with fillets. The spread along the line $p_{st}/p_e = 1$ is probably due to varying effects of end conditions, which become more important as the elastic region is approached. The three models represented by the points on that line all collapsed by elastic general instability.

It may be surprising to note that the presence of fillets appears to have had an important effect on the general instability collapse strength. One might naturally think that the benefits from reducing stress concentrations would be noticeable only in the case of interframe

shell collapse and not for overall collapse. Actually these tests show that the converse was true. Furthermore the maximum shell stresses at the frames were relatively low for the general instability models. In most cases these stresses, according to calculations, were less than the yield stress at the point of collapse. This information plus many additional calculations may be found in the Appendix.

Table 5 lists the models that had local shell failures together with some pertinent theoretical calculations. Expressing these results also in terms of ratios of theoretical to adjusted experimental pressures, Column 2 gives the results for the Lunchick inelastic buckling analysis,[1] which is the only one listed that accounts for strain hardening. The next column lists the results for the Lunchick "plastic hinge" solution[4] which is really applicable only in the case of an elastic, ideally plastic material. However it does take the bending stresses into account whereas the inelastic buckling analysis does not. The other four columns list pressure ratios based on the Hencky-Von Mises yield criterion and the maximum stress (Rankine) criterion as determined at critical locations using the analysis of Pulos and Salerno.[5] These procedures are also applicable only to elastic, ideally plastic materials, but they are included here for purposes of comparison.*

For Model 25-24F, the inelastic buckling analysis of Reference 7 for the nonsymmetric mode rather than the Lunchick analysis[1] was used to compute the pressure ratio in the second column. The last row in the table gives the spread in pressure ratios (maximum-minimum) which should be an indication of the consistency of each method. The Lunchick inelastic buckling analysis scores noticeably better on this basis, as it should, although it appears to be generally nonconservative. The accuracy of this analysis appears to be best for thickest models and poorest for the thinnest. This fact may be considered surprising since the variation in stress through the thickness is not taken into account in the analysis. Pressure ratios in the fifth and sixth columns show that in many cases the bending stresses in the shell were quite high. However they seem not to have seriously affected the collapse strength of the thicker cylinders, as indicated by the pressure ratios for the Lunchick inelastic buckling analysis. On the other hand, the Lunchick plastic hinge analysis appears to overestimate the effects of bending stresses in the thicker cylinders.

The presence of fillets seems to have had little effect on the collapse strength. This can be seen by comparing pressure ratios in Column 2 for comparable models with and without fillets. As previously noted, this fact was thought somewhat surprising, and it may be of considerable importance.

---

*In all stress calculations, the analysis of Pulos and Salerno was modified to consider the external position of the frames and the outside pressure radius. R_o was used in place of the radius to the midplane of the shell, and the frame area was adjusted according to a procedure given in Reference 6. This adjustment gives an equivalent frame area that, when located at the midplane of the shell, has the same capacity to resist radial forces as the actual frame.

These results can probably be seen more clearly by once again making use of a stability ratio diagram. In Figure 5, the abscissa is the ratio of the Lunchick inelastic buckling pressure p_L to the elastic buckling pressure p_e for the axisymmetric mode. The ordinate is the ratio of the adjusted experimental pressure to p_e. The models with thickest shells appear in the lower range (high margin of stability) of p_L/p_e whereas the thinnest shells appear in the upper range. It is quite clear that the accuracy of the Lunchick analysis becomes poorer as p_L/p_e increases. The reason for this is not clear. Since there is no noticeable difference in the performance of the models with fillets and those without, even in the upper range of p_L/p_e, it cannot be said that bending stresses at the frames are responsible for the poor accuracy in this range.

Another possibility is that bending stresses at midbay have important weakening effects (these would not be substantially reduced by the introduction of fillets), but if this is so, the figure would indicate that they are important only in the upper (low stability) range of p_L/p_e. The authors of Reference 8 have recently suggested that this may be the explanation and have devised an empirical correction to the Lunchick solution in efforts to account for it. Their procedure can be represented as follows:

The Lunchick inelastic buckling pressure p_L is based on the membrane stress intensity calculated at midbay. If p_{oL} is defined as the equivalent pressure based on the stress at the outer surface, then $p_{cL} < p_L$ because the stresses at that location are always greater than the membrane stresses; p_L' is the modified Lunchick pressure and is given by:

$$p_L' = p_{oL} + 0.2\left(\frac{p_e}{p_{oL}} - 1.0\right)(p_L - p_{oL})$$

for $$1.0 \leq \frac{p_e}{p_{oL}} \leq 6.0$$

It is seen that when $p_e = p_{oL}$, $p_L' = p_{oL}$, but when $\frac{p_e}{p_{oL}} = 6$, p_L' becomes p_L. This corresponds to a high margin of stability $\left(\frac{p_L}{p_e} = 0.163 \text{ in Figure 5}\right)$. The formula applies only in the stability range stated. For $\frac{p_e}{p_{oL}} > 6.0$, the unmodified Lunchick pressure p_L is to be used.

So far there has not been sufficient time to assess the accuracy of this formula with the present data. However it appears that p_L' should give closer agreement with the tests than does p_L.

DISCUSSION

When considering the results of this investigation (and the general instability data in particular), it is important to realize that the original objectives have imposed definite limitations on the scope of the study. The data presented in Figure 4 cover a wide range of stability ratios, but this should not lead one to conclude that the results represent a complete study of the parameters affecting general instability strength. The total cylinder length L_B, for example, is one of the critical parameters, but it was not adequately covered because it has no importance for local shell buckling. A practical vehicle might be as long as 10 diameters, but the longest cylinder (25-84) represented in Figure 4 is only 2 diameters long. Frame shape, another important factor, has not been included in this study, all frames having been rectangular in cross section. The margin of stability of many of the models probably could have been improved by using more efficient sections, e.g., T-sections having the same weight. Thus the upper range of p_{st}/p_e where agreement between theory and experiment is poorest may be out of the range of practical frame design.

Another consideration is the relative stress distribution in the frames and shell. In each of the analyses evaluated in Table 4, it is assumed that the frames and shell are equally stressed. Calculations show that this is not a bad assumption for the models tabulated, but it is an approximation that becomes less accurate with increasing θ. Thus for larger values of θ than those investigated, it is possible that the shell could be stressed well into the inelastic region before the frame stresses have reached the elastic limit. Such cases might be studied with longer cylinders.

The position of the frame is another factor to be considered. It is shown in Reference 6 that internal frames absorb a greater share of the total load on a section than do external frames of the same cross section. However, in all of the inelastic general instability calculations tabulated here, the location of the frames is not taken into account in the computation of stress. That is, the stress intensity used to determine the reduced moduli E_s and E_t is obtained with the frame area taken to be concentrated at the shell radius. Consequently it might be expected that buckling pressures for a corresponding series of internally framed cylinders would be somewhat higher and therefore in better agreement with the calculations.

By what mechanism the presence of fillets increases inelastic general instability strength is a question not likely to be answered with the results at hand. Perhaps some additional tests using duplicates of a few selected models but with strain measurements taken on and near the frames would provide informative data. It is significant to note, however, that an actual welded structure would have fillets and that it is these cases in which theory and experiment are in best agreement.

In view of the small number of shell buckling failures observed, the data for this mode of collapse also appear to be insufficient for a complete evaluation of the Lunchick analysis. In particular, Figure 5 shows a conspicuous gap in the range $0.2 < p_c/p_e < 0.35$. This could probably be filled in with some additional cylinders having h/R in the range 0.03–0.04. It has also been pointed out that calculated midbay bending stresses for all models shown in Figure 5 were relatively large and that they may be responsible for the poor correlation in the upper range of p_l/p_e. To determine the validity of this suspicion, data are therefore needed for models having the same range of p_l/p_e but with relatively low bending stresses. This might be accomplished through the use of shorter models having lighter frames but with T-cross sections to prevent general instability collapse.

It is also worth noting that the group of models at the upper end of the p_l/p_e scale probably do not represent realistic designs. The high bending stresses would no doubt be unacceptable for a practical vehicle because of the possibility of fatigue and necessary allowances for the presence of residual stresses and imperfections. It is therefore more likely that lighter frames with closer spacings would be used, thereby reducing θ and consequently decreasing p_l/p_e. Weight considerations would naturally require the use of a more efficient frame shape such as the T so that further reductions in frame size would be possible. Use of p_l in the design of a practical vehicle is therefore not apt to be required in the range where its reliability is poorest.

Finally, it should be emphasized that these models were relatively free of the weakening influences of imperfections and residual stresses inherent in structures fabricated by conventional techniques. Any conclusions as to the reliability of the various analyses for the design of full-scale hulls must therefore await tests of models in which such effects can be studied.

CONCLUSIONS

The following statements apply only for near-perfect cylinders made of strain-hardening materials and stiffened by external rings.

1. The present series of tests provide useful data on inelastic buckling in the axisymmetric and general instability modes but not enough, however, for a full evaluation of relevant theory.

2. For the two buckling modes, the analyses of Lunchick[1,2] and Krenzke and Kiernan[3] are likely to be unconservative in their predictions of collapse strength, when fillets are not employed but should improve in accuracy as p_c/p_e is reduced.

3. The presence of high bending stresses near the frames did not noticeably affect the axisymmetric shell buckling strength for the models tested.

4. Inelastic general instability strength in the range $0.5 < p_c/p_e < 1.0$ can be increased significantly by the introduction of frame fillets even though bending stresses in the vicinity of the frames are relatively low when fillets are absent.

ACKNOWLEDGMENT

The authors are indebted to Mr. Martin A. Krenzke who conceived the general approach followed in these studies.

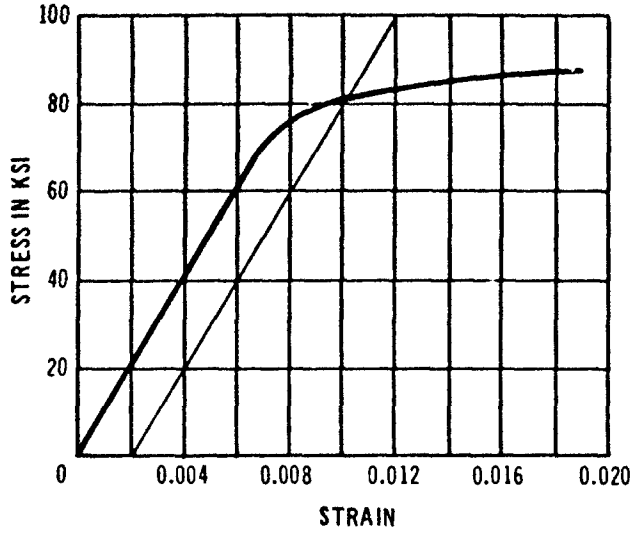

Figure 1a – Stress-Strain Curve

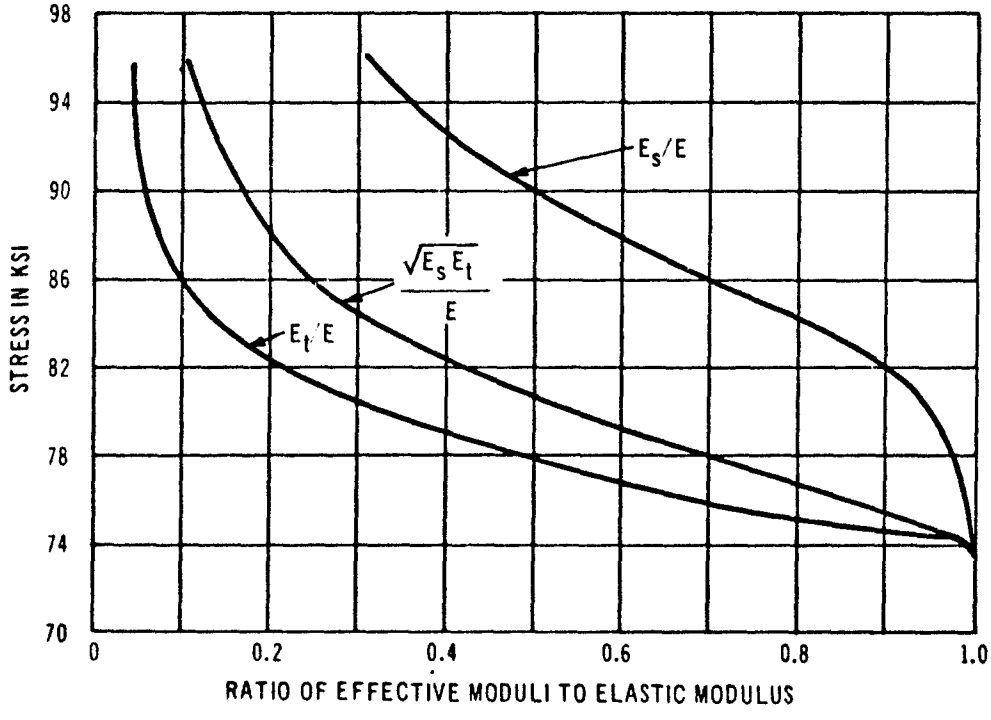

Figure 1b – Effective Modulus Plots

Figure 1 – Typical Data on Material Properties of 7075-T6 Aluminum

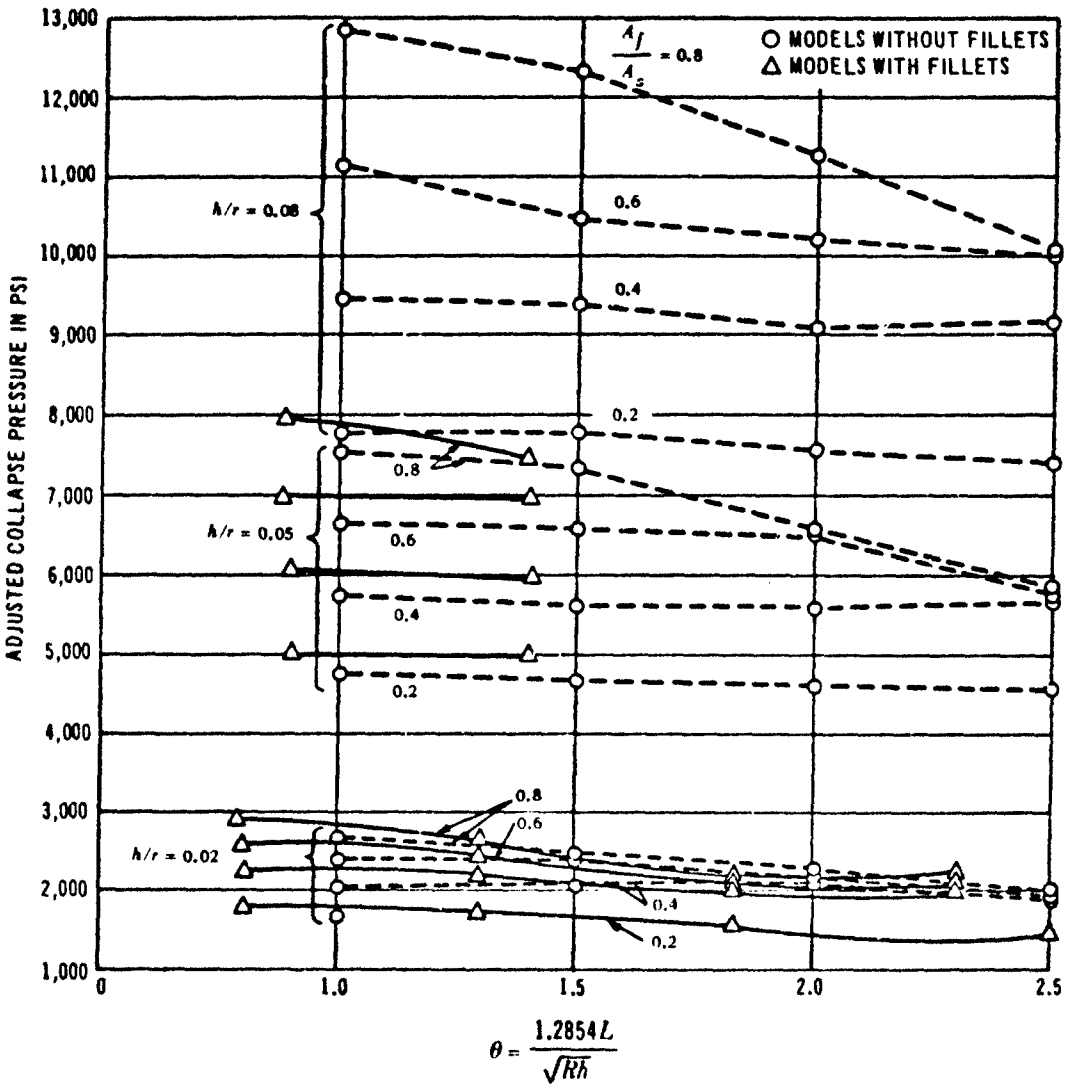

Figure 2 – Effects of Parametric Variations on Adjusted Experimental Collapse Pressures

Figure 3 – Models after Collapse

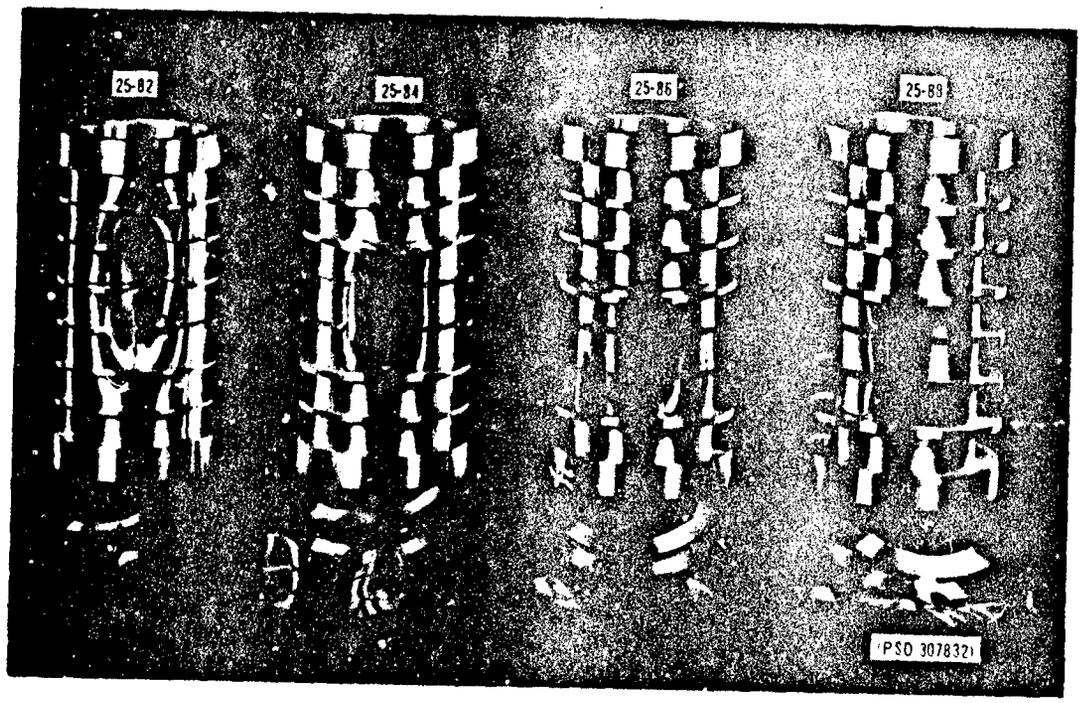

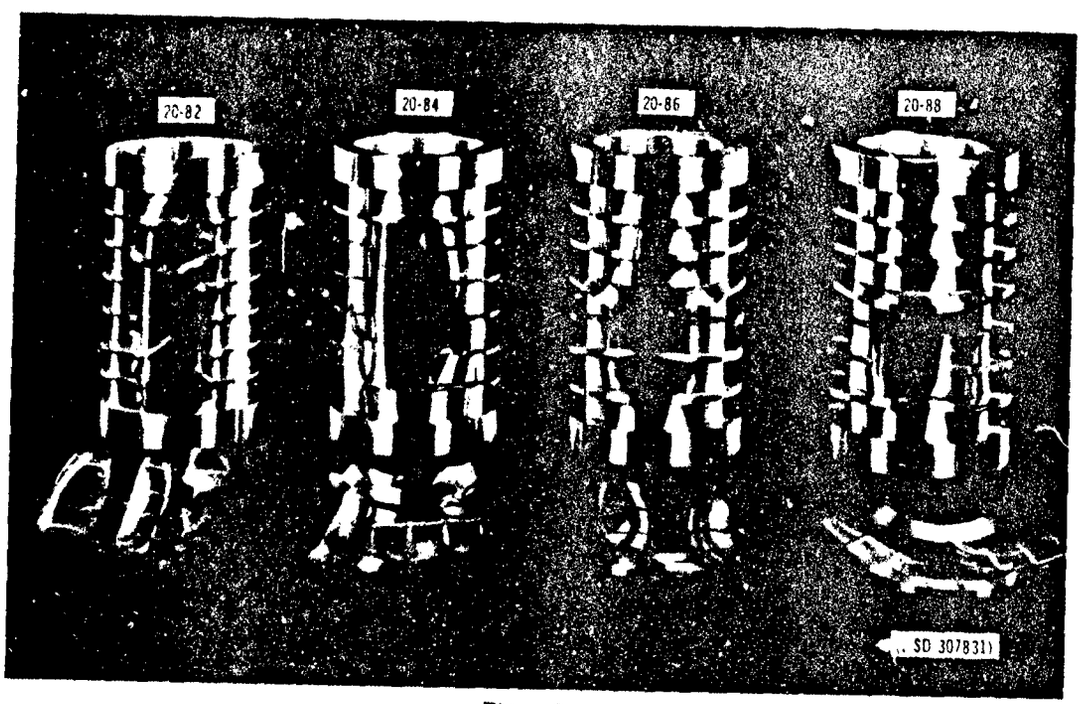

Figure 3a

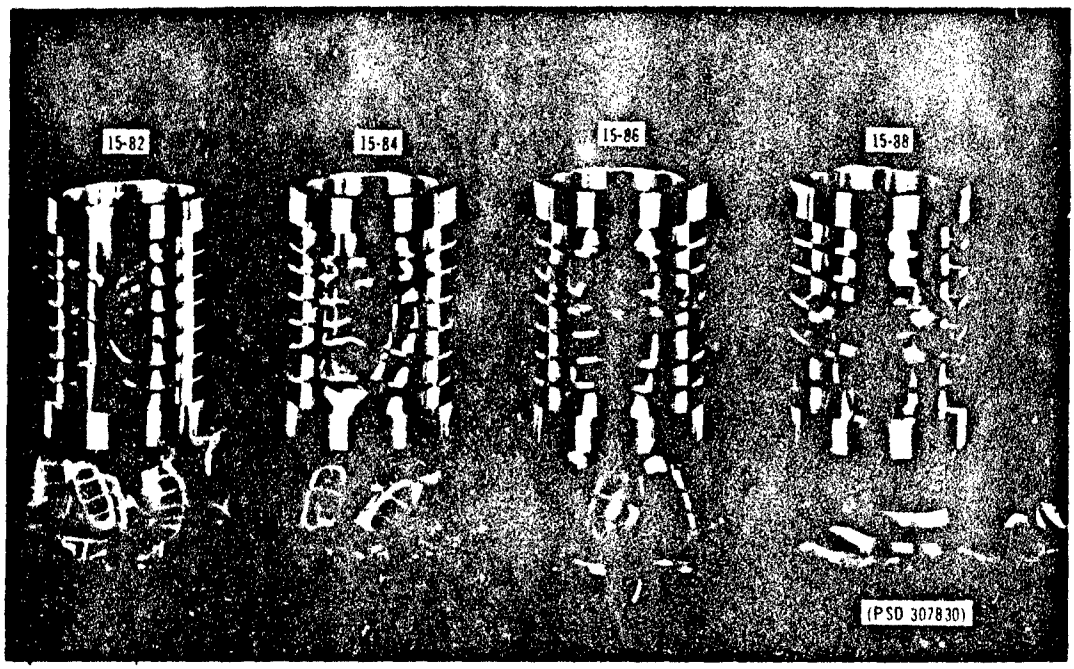
15-82
15-84
15-86
15-88
(PSD 307830)

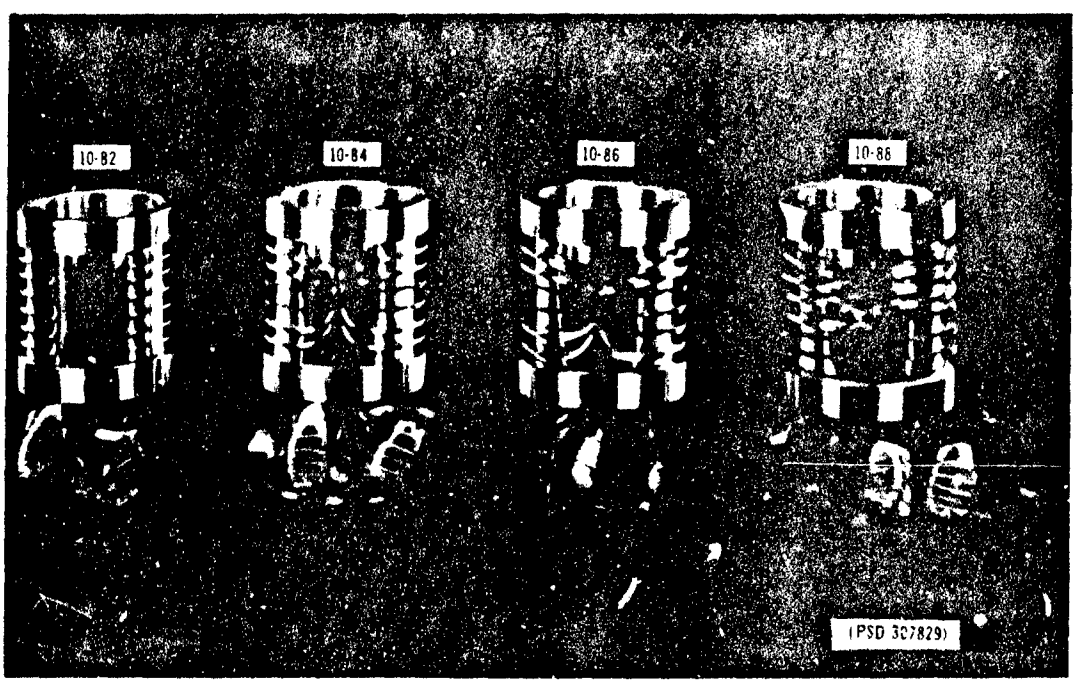
10-82
10-84
10-86
10-88
(PSD 307829)

Figure 3b

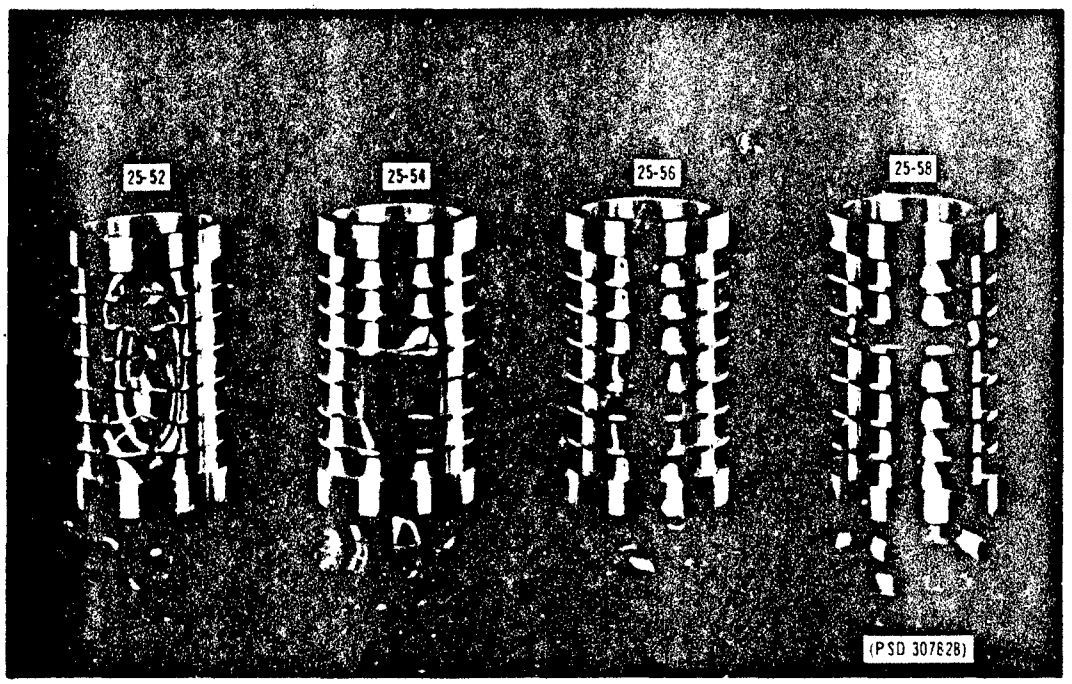
25-52
25-54
25-56
25-58
(PSD 307828)

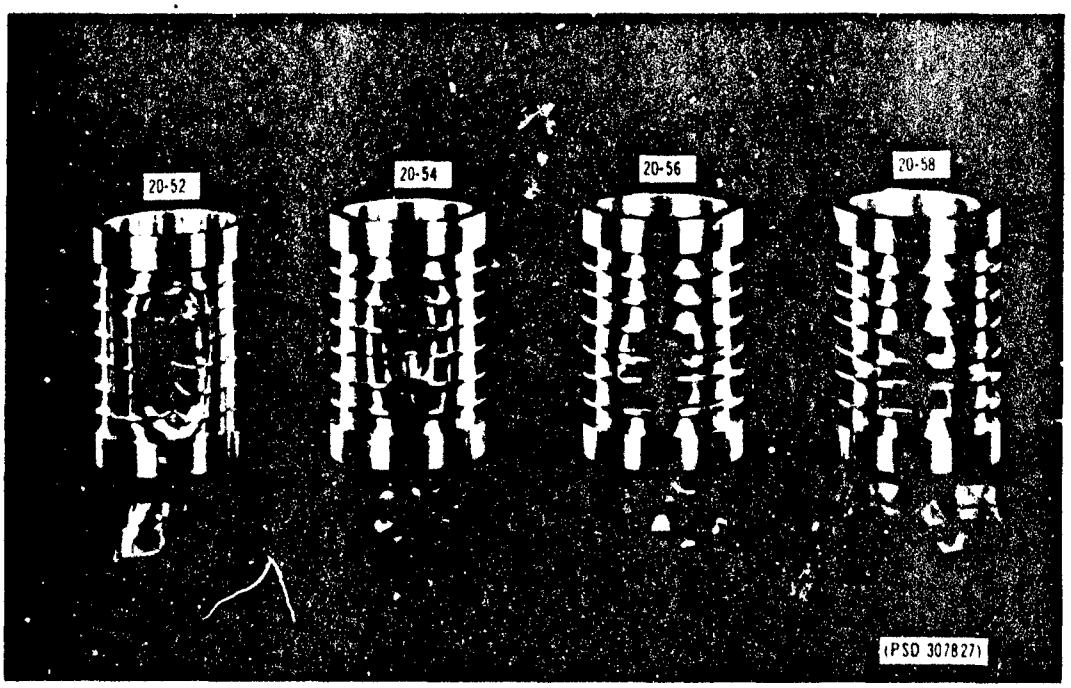
20-52
20-54
20-56
20-58
(PSD 307827)

Figure 3c

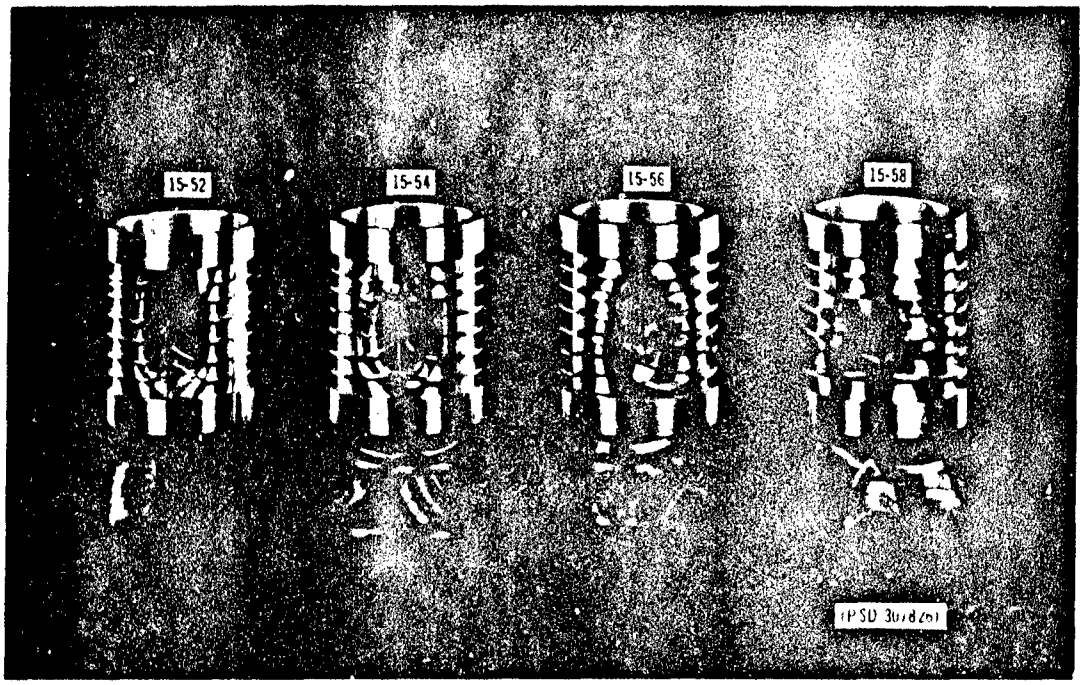

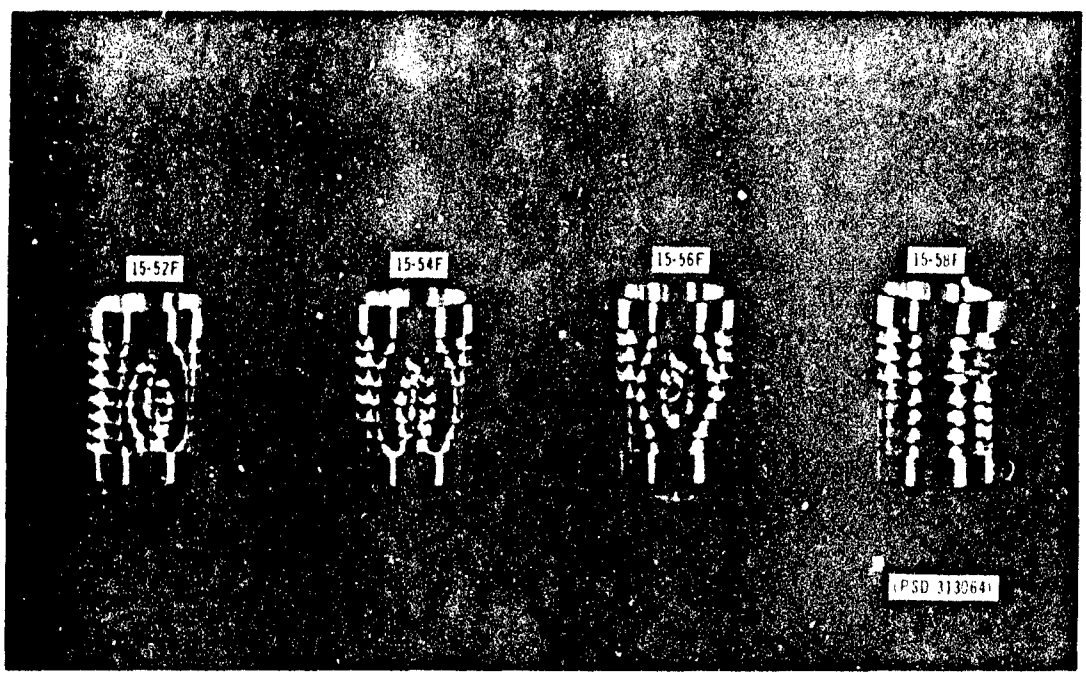

Figure 3d

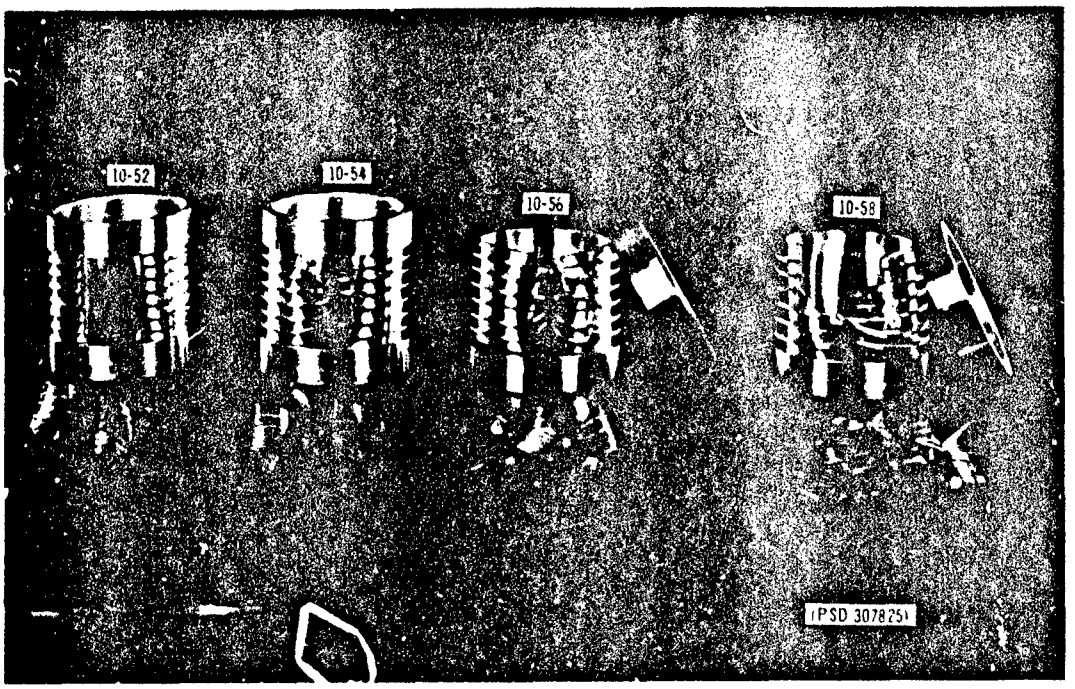
10-52
10-54
10-56
10-58
(PSD 307825)

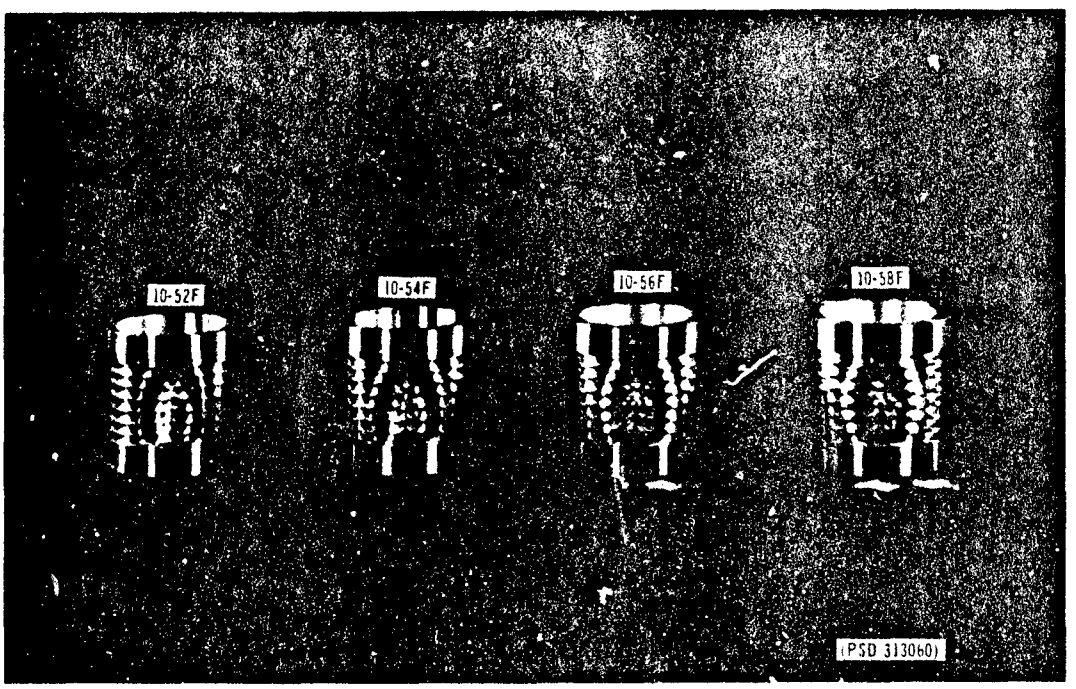
10-52F
10-54F
10-56F
10-58F
(PSD 313060)

Figure 3e

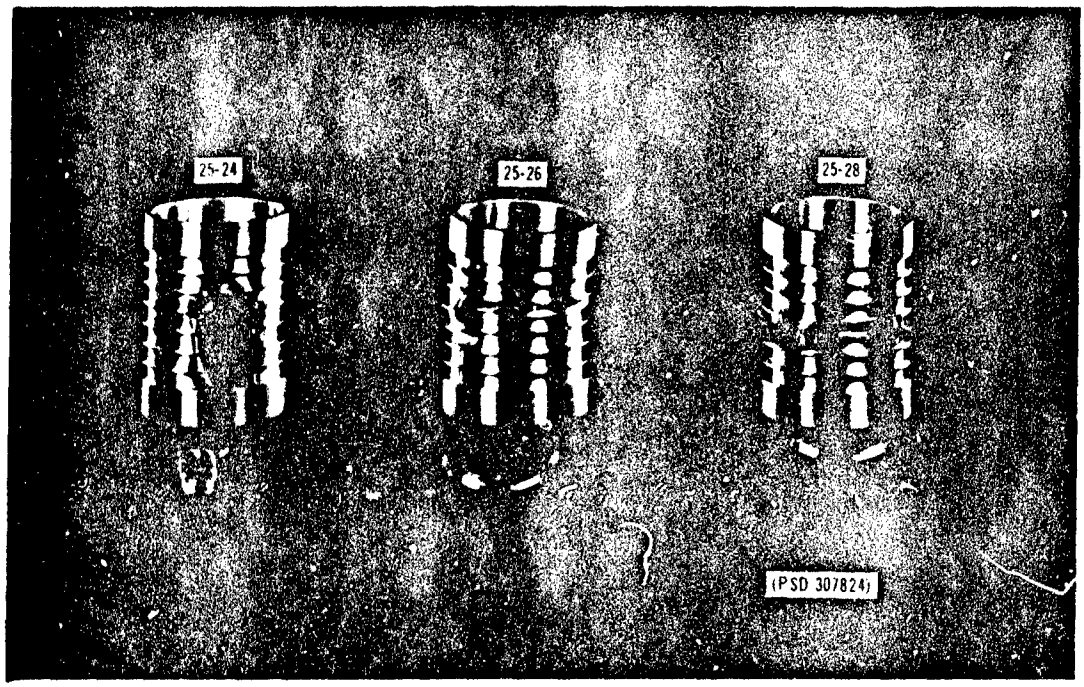
25-24
25-26
25-28
(PSD 307824)

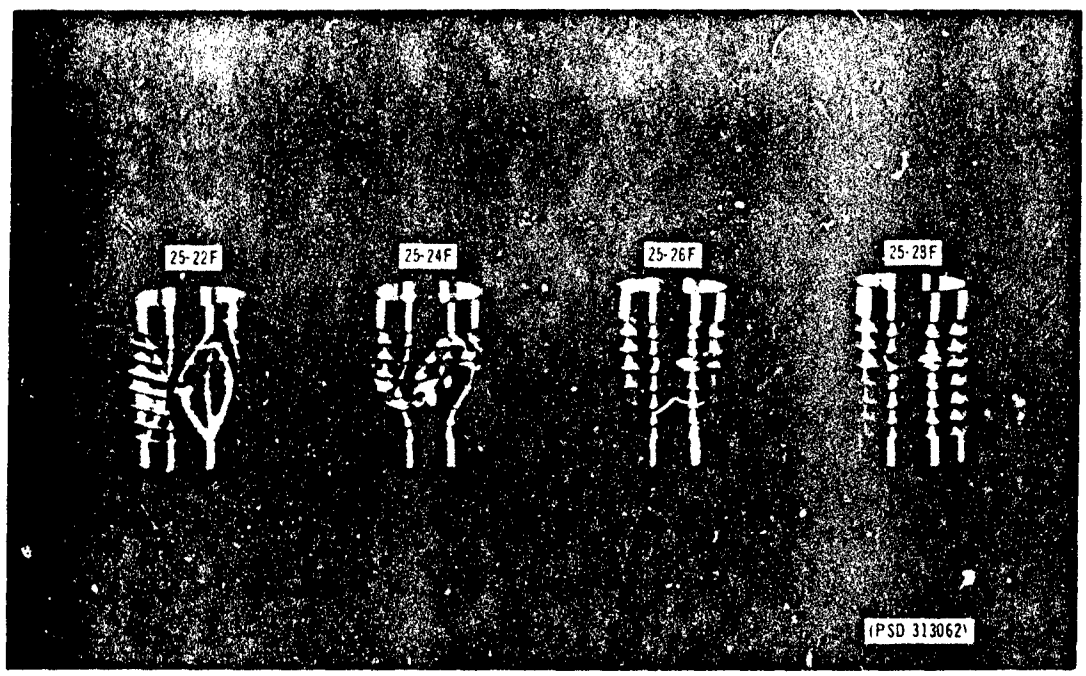
25-22F
25-24F
25-26F
25-28F
(PSD 313062)

Figure 3f

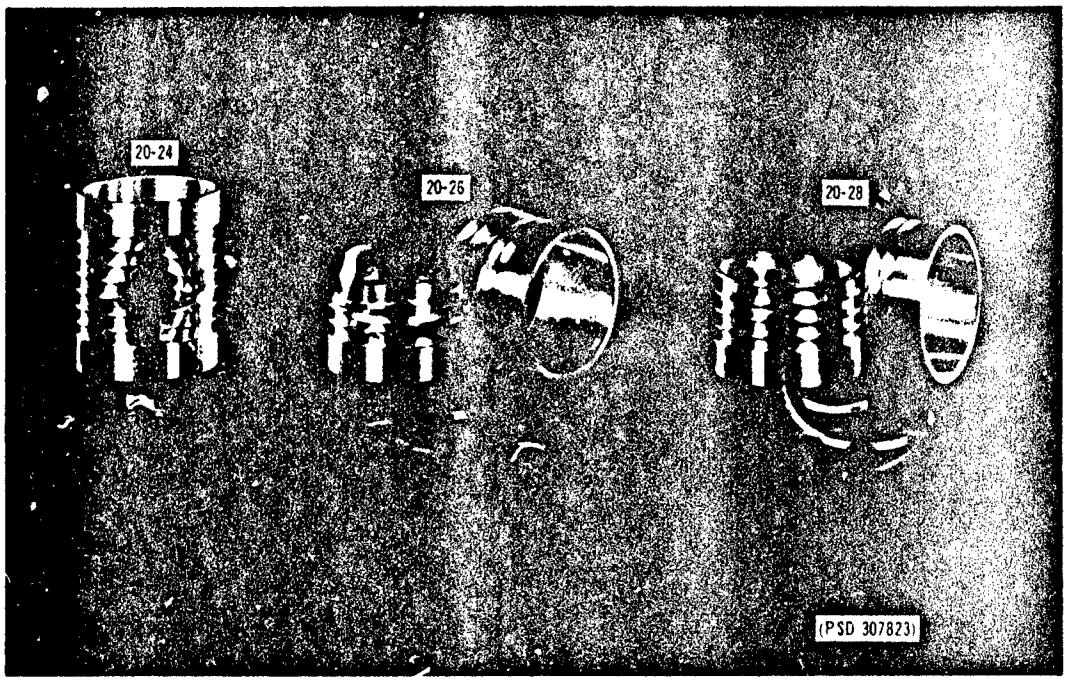
20-24
20-26
20-28
(PSD 307823)

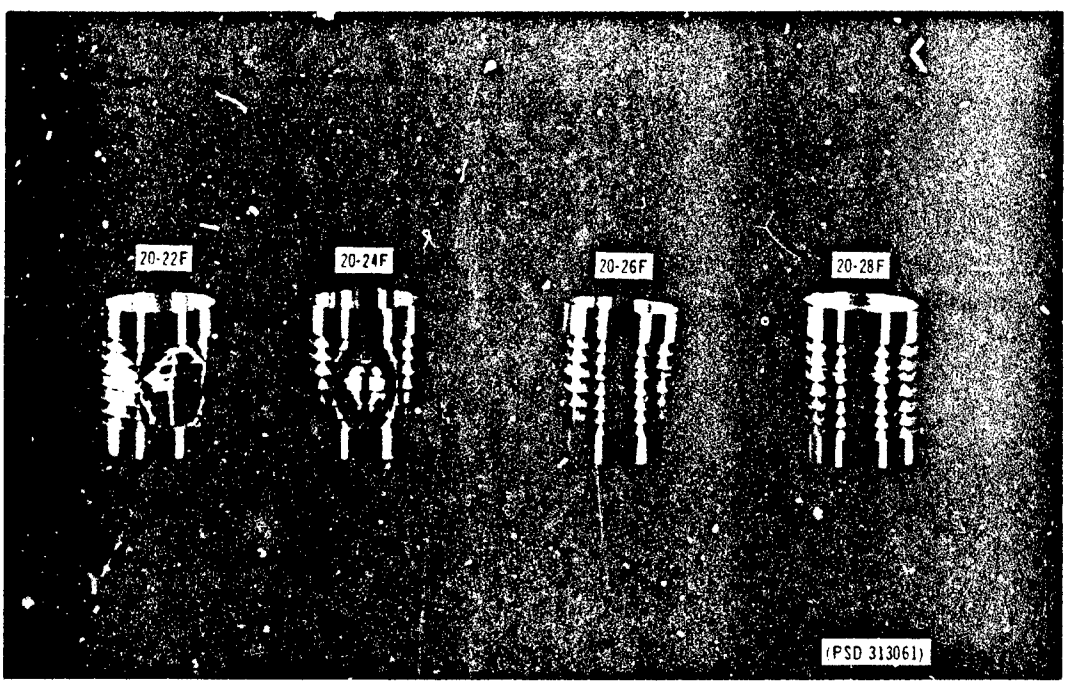
20-22F
20-24F
20-26F
20-28F
(PSD 313061)

Figure 3g

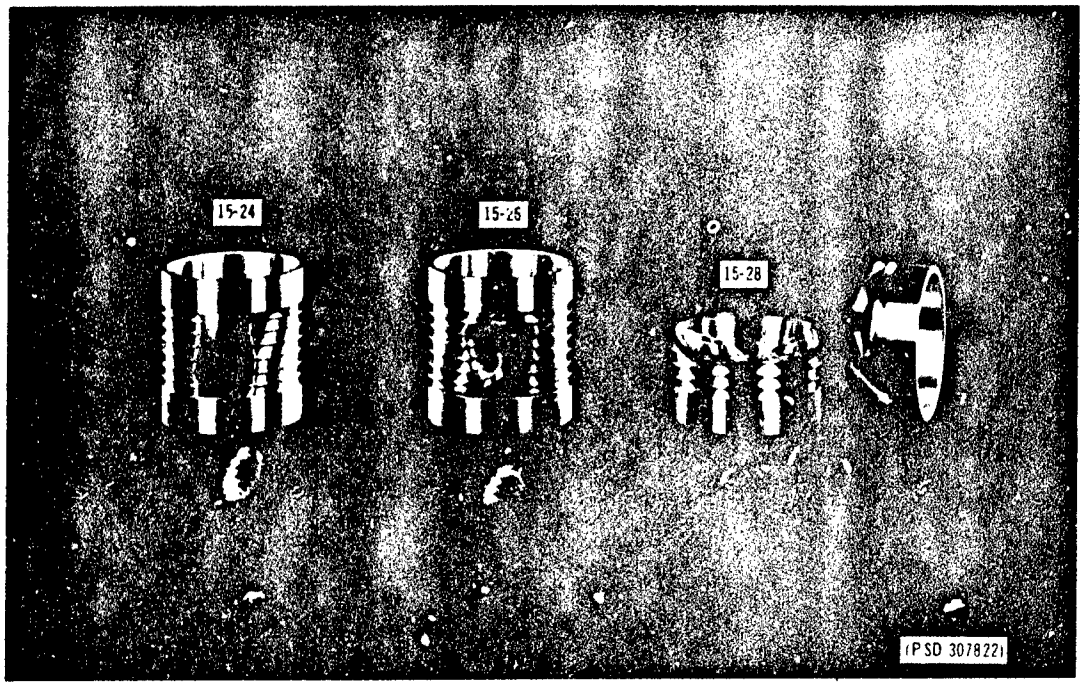
15-24
15-26
15-28
(PSD 307822)

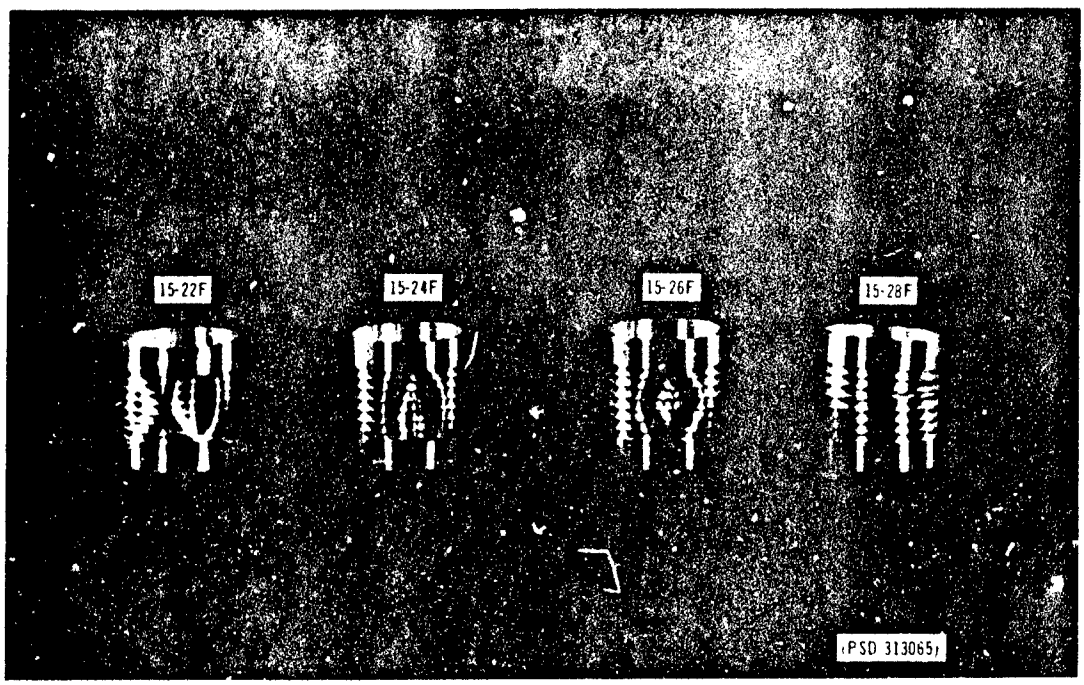
15-22F
15-24F
15-26F
15-28F
(PSD 313065)

Figure 3h

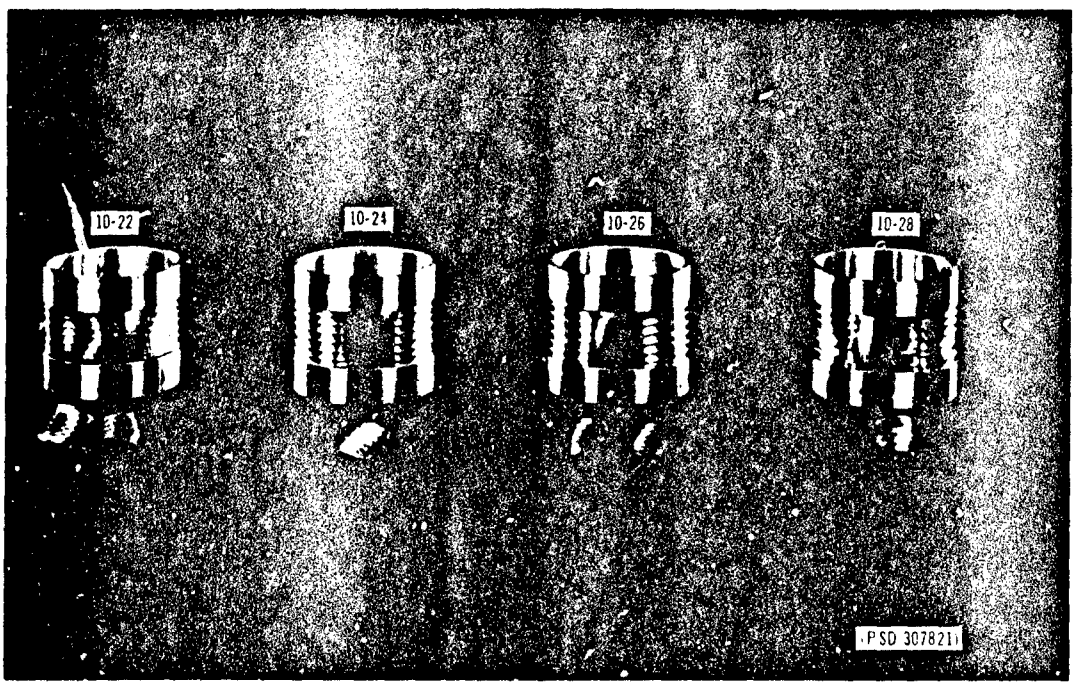
10-22
10-24
10-26
10-28
PSD 307821

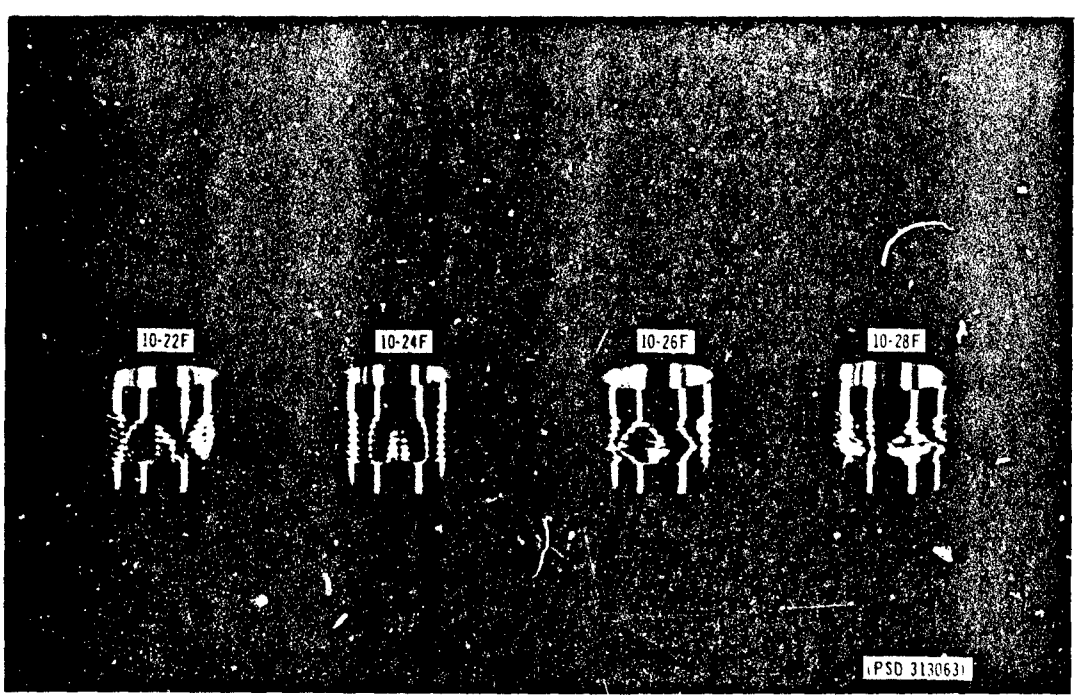
10-22F
10-24F
10-26F
10-28F
PSD 313063

Figure 31

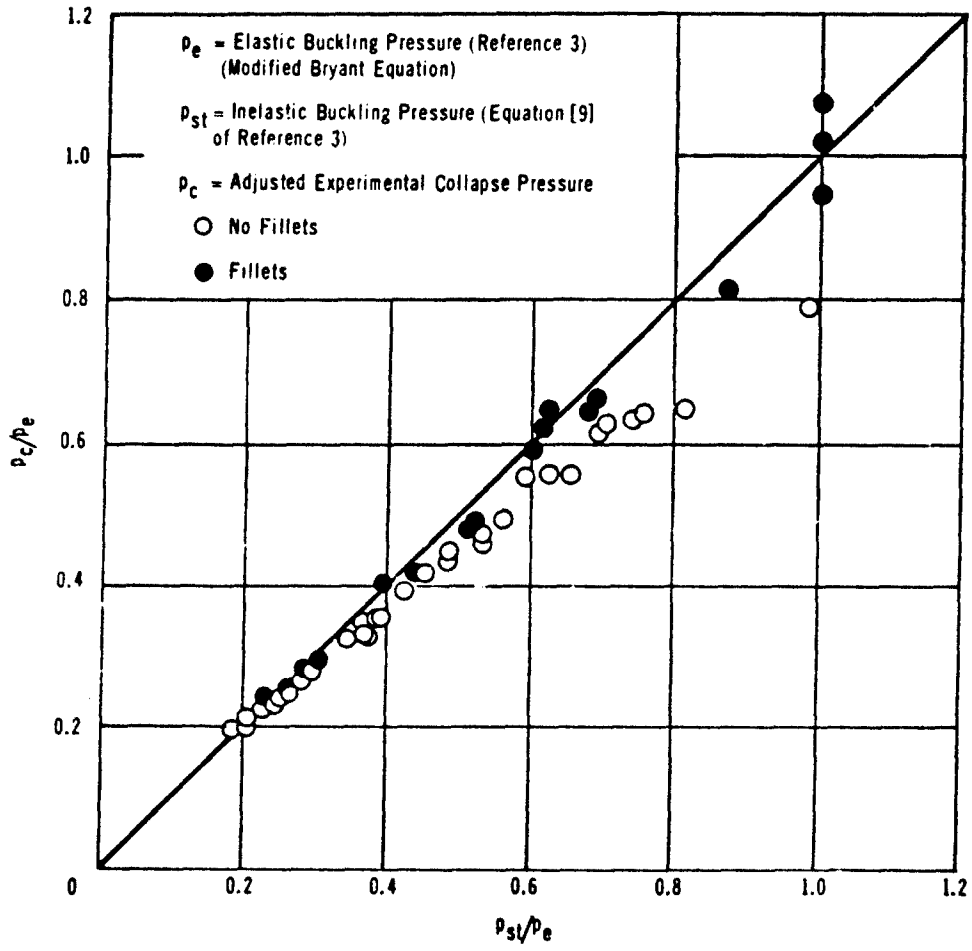

Figure 4 – General Instability Data Compared with Results of Krenzke-Kiernan Analysis

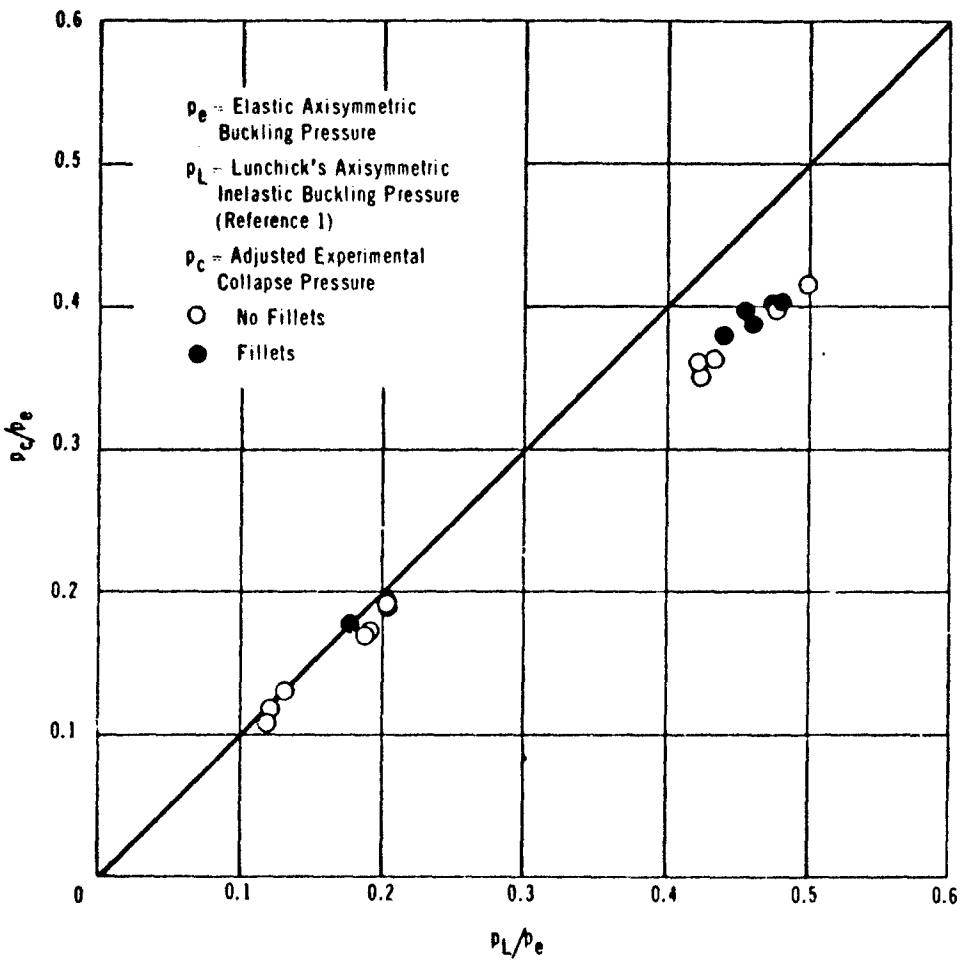

Figure 5 – Axisymmetric Shell Buckling Data Compared with Results of Lunchick Analysis

TABLE 1

Measured Model Dimensions and Yield Strengths

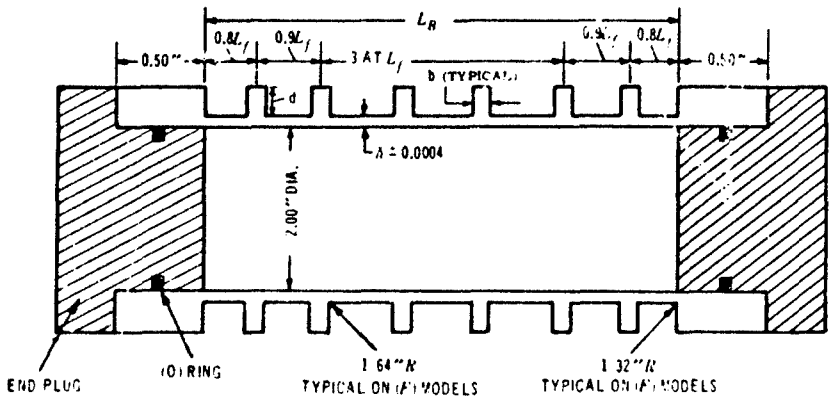

Model	L_f	b	h	d	L_B	Compressive Yield Strength (0.2% Offset) psi
25-88	0.699	0.127	0.0830	0.386	4.473	80,600
25-86	0.679	0.107	0.0832	0.318	4.349	80,600
25-84	0.659	0.086	0.0830	0.255	4.216	80,700
25-82	0.632	0.059	0.0825	0.179	4.047	80,700
20-88	0.572	0.112	0.0830	0.340	3.647	80,700
20-86	0.555	0.097	0.0830	0.287	3.552	80,700
20-84	0.537	0.079	0.0830	0.230	3.430	81,400
20-82	0.511	0.054	0.0832	0.158	3.280	82,000
15-88	0.444	0.100	0.0830	0.297	2.843	82,700
15-86	0.428	0.084	0.0830	0.253	2.745	82,700
15-84	0.413	0.068	0.0830	0.202	2.638	83,000
15-82	0.390	0.046	0.0830	0.140	2.502	83,300
10-88	0.313	0.084	0.0833	0.246	2.002	83,500
10-86	0.300	0.071	0.0830	0.211	1.920	83,500
10-84	0.286	0.057	0.0830	0.167	1.830	83,400
10-82	0.269	0.039	0.0833	0.115	1.715	83,200
25-58	0.532	0.086	0.0513	0.254	3.405	83,000
25-56	0.520	0.074	0.0510	0.217	3.327	83,000
25-54	0.506	0.060	0.0513	0.174	3.239	83,200
25-52	0.487	0.042	0.0511	0.123	3.117	83,400
20-58	0.434	0.071	0.0513	0.232	2.778	83,600
20-56	0.424	0.067	0.0513	0.194	2.715	83,600
20-54	0.410	0.053	0.0511	0.159	2.624	83,400
20-52	0.394	0.037	0.0511	0.110	2.522	83,300
15-58	0.337	0.069	0.0506	0.201	2.157	83,200
15-56	0.326	0.058	0.0513	0.174	2.085	83,200
15-54	0.315	0.047	0.0513	0.138	2.017	83,400
15-52	0.300	0.032	0.0514	0.097	1.919	82,500
10-58	0.235	0.057	0.0515	0.169	1.506	83,700
10-56	0.226	0.048	0.0511	0.146	1.446	83,700
10-54	0.217	0.040	0.0516	0.114	1.389	83,800
10-52	0.205	0.027	0.0518	0.078	1.311	84,100
25-28	0.320	0.043	0.0200	0.123	2.049	78,400
25-26	0.314	0.036	0.0204	0.106	2.008	80,600
25-24	0.307	0.030	0.0202	0.086	1.965	84,300

Model	L_f	b	h	d	L_B	Compressive Yield Strength (0.2% Offset) psi
20-28	0.260	0.038	0.0203	0.111	1.661	84,300
20-26	0.253	0.032	0.0204	0.096	1.626	84,400
20-24	0.248	0.026	0.0210	0.076	1.586	84,400
15-28	0.200	0.033	0.0201	0.099	1.280	84,000
15-26	0.196	0.029	0.0205	0.081	1.254	83,800
15-24	0.190	0.023	0.0206	0.066	1.216	83,500
10-28	0.140	0.028	0.0206	0.079	0.888	83,500
10-26	0.135	0.024	0.0205	0.068	0.863	83,500
10-24	0.130	0.019	0.0203	0.056	0.834	83,600
10-22	0.124	0.014	0.0203	0.039	0.793	83,600
15-58F	0.337	0.067	0.0511	0.200	2.157	82,000
15-56F	0.325	0.056	0.0507	0.174	2.087	82,000
15-54F	0.313	0.042	0.0512	0.134	2.018	82,000
15-52F	0.300	0.030	0.0510	0.097	1.921	82,000
10-58F	0.235	0.055	0.0515	0.169	1.506	82,000
10-56F	0.225	0.047	0.0517	0.145	1.446	82,500
10-54F	0.216	0.036	0.0510	0.109	1.390	82,900
10-52F	0.205	0.025	0.0509	0.079	1.315	83,400
25-28F	0.320	0.040	0.0200	0.122	2.048	83,400
25-26F	0.310	0.030	0.0209	0.105	2.010	82,800
25-24F	0.307	0.029	0.0200	0.086	1.967	82,300
25-22F	0.298	0.019	0.0205	0.060	1.910	81,700
20-28F	0.260	0.036	0.0193	0.112	1.665	81,700
20-26F	0.253	0.030	0.0193	0.097	1.626	81,300
20-24F	0.247	0.026	0.0199	0.077	1.588	80,800
20-22F	0.241	0.018	0.0197	0.054	1.538	80,400
15-28F	0.199	0.033	0.0207	0.097	1.278	80,400
15-26F	0.196	0.028	0.0204	0.081	1.255	81,100
15-24F	0.190	0.023	0.0208	0.067	1.217	81,700
15-22F	0.183	0.016	0.0203	0.049	1.173	82,400
10-28F	0.139	0.028	0.0213	0.079	0.889	82,400
10-26F	0.137	0.027	0.0202	0.068	0.861	82,300
10-24F	0.130	0.019	0.0199	0.057	0.832	82,300
10-22F	0.125	0.015	0.0200	0.039	0.795	82,200

TABLE 2

Experimental Collapse Data

Model	Experimental Collapse Pressures		Mode of Collapse
	Observed	Adjusted*	
25-88	9,450	10,061	Axisymmetric
25-86	9,550	9,991	Axisymmetric
25-84	8,950	9,123	I.G.I.†
25-82	7,275	7,388	I.G.I.
20-88	10,600	11,251	Axisymmetric
20-86	9,750	10,201	I.G.I.
20-84	8,800	9,072	I.G.I.
20-82	7,400	7,515	I.G.I.
15-88	11,600	12,316	I.G.I.
15-86	10,000	10,458	I.G.I.
15-84	9,100	9,380	I.G.I.
15-82	7,650	7,766	I.G.I.
10-88	12,100	12,846	I.G.I.
10-86	10,650	11,140	I.G.I.
10-84	9,150	9,432	I.G.I.
10-82	7,650	7,767	I.G.I.
25-58	5,600	5,818	Axisymmetric
25-56	5,600	5,764	Axisymmetric
25-54	5,550	5,659	I.G.I.
25-52	4,470	4,515	I.G.I.
20-58	6,300	6,546	Axisymmetric
20-56	6,300	6,484	Axisymmetric
20-54	5,450	5,557	I.G.I.
20-52	4,500	4,545	I.G.I.
15-58	7,050	7,326	I.G.I.
15-56	6,400	6,588	I.G.I.
15-54	5,500	5,607	I.G.I.
15-52	4,600	4,645	I.G.I.
10-58	7,250	7,538	I.G.I.
10-56	6,450	6,640	I.G.I.
10-54	5,625	5,738	I.G.I.
10-52	4,700	4,746	I.G.I.
25-28	1,850	1,883	Axisymmetric**
25-26	1,960	1,992	Axisymmetric**
25-24	1,980	1,895	I.G.I.
20-28	2,225	2,260	Axisymmetric
20-26	2,150	2,176	Axisymmetric
20-24	2,075	2,091	I.G.I.
15-28	2,400	2,438	Axisymmetric
15-26	2,360	2,388	I.G.I.
15-24	2,060	2,076	I.G.I.
10-28	2,625	2,666	I.G.I.
10-26	2,360	2,388	I.G.I.
10-24	2,040	2,056	I.G.I.
10-22	1,640	1,647	I.G.I.
15-58F	7,400	7,681	Axisymmetric
15-56F	6,750	5,943	I.G.I.
15-54F	5,850	5,953	I.G.I.
15-52F	4,920	4,965	I.G.I.
10-58F	7,700	7,989	I.G.I.
10-56F	6,800	6,996	I.G.I.
10-54F	5,950	6,080	I.G.I.
10-52F	5,000	5,031	I.G.I.
25-28F	2,160	2,192	Axisymmetric
25-26F	2,080	2,100	Axisymmetric
25-24F	1,935	1,950	Nonsymmetric
25-22F	1,420	1,425	E.G.I.††
20-28F	2,135	2,167	Axisymmetric
20-26F	2,100	2,124	Axisymmetric
20-24F	2,060	2,076	I.G.I.
20-22F	1,520	1,526	E.G.I.
15-28F	2,580	2,621	Axisymmetric
15-26F	2,400	2,427	I.G.I.
15-24F	2,180	2,197	I.G.I.
15-22F	1,720	1,727	E.G.I.
10-28F	2,840	2,884	I.G.I.**
10-26F	2,540	2,574	I.G.I.**
10-24F	2,180	2,198	I.G.I.
10-22F	1,775	1,783	I.G.I.

*Adjusted pressure $= \text{observed pressure} \times \dfrac{\left[L + \dfrac{R_{of}}{R_o} b\right]}{L_f}$

where R_{of} is the radius to outer surface of frame and other terms are as defined previously.

**Buckling mode not clearly distinguishable.

†Inelastic General Instability.

††Elastic General Instability.

TABLE 3

Collapse Mode Distribution

$\frac{A_f}{hL_f}$ / n	h/R = 0.08				h/R = 0.05				h/R = 0.02			
	0.8	0.6	0.4	0.2	0.8	0.6	0.4	0.2	0.8	0.6	0.4	0.2
2.5	1*	1	1	1	2	2	1	2	3 3F	3 3F	3 1F	1F
2.0	1	1	1	2	1	1	2	2	3 3F	3 2F	3 1F	1F
1.5	1	1	1	1	1 1F	1 1F	1 1F	2 1F	3 3F	2 1F	3 1F	1F
1.0	1	1	1	1	1 1F	1 1F	1 1F	2 1F	2 1F	2 1F	3 1F	3 1F

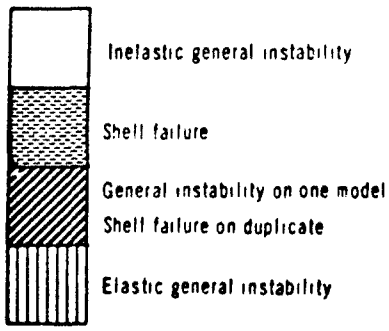

*1 Calculations within 10 percent of test data.
2 Calculations and test data differ by 10-15 percent.
3 Calculations and test data differ by more than 15 percent.

Both designations within a square indicate a duplicated model, the F signifying the one with fillet radii.

TABLE 4

General Instability Data

Model	Ratio of Theoretical to Adjusted Experimental Collapse Pressure			
	Lunchick (Reference 2)	Krenzke-Kiernan (Reference 3)		Average Circumferential Yield p_a
		p_i	p_{st}	
25-84	1.04	1.02	1.04	0.95
25-82	1.08	1.05	1.07	1.00
20-86	1.06	1.03	1.04	0.97
20-84	1.08	1.04	1.06	0.97
20-82	1.15	1.08	1.11	1.01
15-88 *	1.00	0.96	0.98	0.93
15-86	1.09	1.03	1.05	0.97
15-84	1.10	1.03	1.06	0.95
15-82	1.08	1.07	1.07	0.99
10-88	0.99	0.93	0.96	0.90
10-86	1.06	1.02	1.03	0.92
10-84	1.06	1.04	1.05	0.95
10-82	1.11	1.07	1.09	0.99
25-54	1.11	1.06	1.08	1.01
25-52	1.13	1.12	1.12	1.08
20-54	1.10	1.10	1.12	1.02
20-52	1.13	1.11	1.12	1.07
15-58	1.07	1.01	1.03	0.99
15-56	1.06	1.05	1.05	0.99
15-54	1.10	1.09	1.09	1.02
15-52	1.14	1.11	1.12	1.06
10-58	1.02	1.00	1.01	0.98
10-56	1.08	1.03	1.05	0.98
10-54	1.12	1.08	1.10	1.01
10-52	1.13	1.11	1.12	1.05
25-24	1.26	1.24	1.25	1.24
20-24	1.19*	1.17	1.17	1.15
15-26	1.15	1.13	1.14	1.12
15-24	1.17	1.16	1.16	1.13
10-28 *	1.16	1.12	1.12	1.12
10-26	1.16	1.14	1.15	1.14
10-24	1.17	1.16	1.17	1.13
10-22	1.24	1.24	1.24	1.23
15-56F	0.99	0.97	0.98	0.91
15-54F	1.00	0.97	0.98	0.91
15-52F	1.01	0.97	0.99	0.95
10-58F	0.96	0.93	0.94	0.89
10-56F	1.01	0.98	0.99	0.92
10-54F	1.07	1.01	1.04	0.96
10-52F	0.98	0.95	0.96	0.91
25-22F**	0.93	0.93	0.93	
20-24F	1.06	0.98	1.05	1.07
20-22F**	0.98	0.98	0.98	
15-26F	1.06	1.04	1.05	1.05
15-24F	1.06	1.03	1.04	1.05
15-22F**	1.06	1.06	1.06	
10-28F*	1.06	1.03	1.04	1.04
10-26F*	1.07	1.03	1.06	1.05
10-24F	1.02	1.02	1.02	1.03
10-22F	1.07	1.07	1.07	1.12

*Buckling mode not clearly distinguishable.

**Elastic buckling.

TABLE 5

Axisymmetric Shell Buckling Data

Model	Ratio of Theoretical to Adjusted Experimental Collapse Pressure					
	Lunchick Inelastic Buckling (Reference 1) p_L	Lunchick Plastic Hinge (Reference 4)	Hencky-Von Mises Midbay Stresses*		Maximum Stress*	
			Middle Thickness	Exterior	σ_x Inside at Frame	σ_ϕ Outside at Midbay
25-88	1.04	0.86	0.92	0.77	0.61	0.74
25-86	1.05	0.85	0.89	0.78	0.68	0.73
20-88	1.00	0.82	0.86	0.75	0.65	0.71
25-58	1.11	0.98	1.04	0.86	0.68	0.85
25-56	1.11	0.96	1.01	0.87	0.73	0.82
20-58	1.05	0.93	0.99	0.84	0.72	0.82
20-56	1.06	0.90	0.95	0.83	0.77	0.79
25-28 †	1.21	1.13	1.23	0.96	0.75	1.01
25-26 †	1.17	1.09	1.17	0.96	0.83	0.97
20-28	1.20	1.13	1.21	0.99	0.82	1.01
20-26	1.20	1.16	1.20	1.05	0.93	1.00
15-28	1.19	1.10	1.15	1.02	0.91	0.99
15-58F	0.99	0.83	0.85	0.79	0.75	0.74
25-28F	1.19	1.10	1.19	0.96	0.80	0.98
25-26F	1.19	1.10	1.12	1.00	0.93	0.96
25-24F	1.10**	1.11	1.16	1.03	0.99	0.96
20-28F	1.17	1.09	1.17	0.98	0.84	0.98
20-26F	1.15	1.07	1.12	0.98	0.91	0.94
15-28F	1.16	1.02	1.05	0.96	0.92	0.91
Spread	0.21	0.34	0.38	0.30	0.38	0.30

*Stresses calculated using analysis of Pulos and Salerno.[5]

**Nonsymmetric shell buckling. Theoretical collapse pressure in this column obtained from analysis of Reference 7.

†Buckling mode not clearly distinguishable.

APPENDIX

SUMMARY OF TEST RESULTS

or reference purposes, a comprehensive tabulation of all test results and calculations led here as Table 6.

TABLE 3

Summary of Test Results and Calculations

Model	Ratio of Theoretical to Adjusted Expe																	
	25-88	25-86	25-84	25-82	20-88	20-86	20-84	20-82	15-88	15-86	15-84	15-82	10-88	10-86	10-84	10-82	25-58	25-5(
m Stress Criterion																		
itudinal, Frame	0.61	0.68	0.82	1.19	0.65	0.77	0.95	1.32	0.73	0.90	1.07	1.42	0.84	0.99	1.21	1.54	0.68	0.7
ferential, Midbay	0.74	0.73	0.76	0.89	0.71	0.75	0.81	0.92	0.71	0.79	0.83	0.92	0.72	0.78	0.85	0.93	0.85	0.8
cky-Von Mises ess Criterion																		
bay, Midplane	0.92	0.89	0.92	1.06	0.86	0.90	0.97	1.09	0.83	0.93	0.97	1.07	0.82	0.89	0.98	1.08	1.04	1.0
dbay, Outside	0.77	0.78	0.84	1.02	0.75	0.80	0.90	1.05	0.77	0.87	0.93	1.05	0.79	0.87	0.96	1.07	0.86	0.8
ck Plastic Hinge[4]	0.86	0.85	0.89	1.05	0.82	0.86	0.94	1.07	0.81	0.90	0.95	1.06	0.81	0.89	0.97	1.08	0.98	0.9
c Shell Buckling																		
ymmetric Mode[7]	5.37	5.21	5.48	6.23	6.31	6.86	7.39	8.52	8.37	9.66	10.34	12.10	13.86	15.89	18.98	23.18	3.61	3.4
nmetric Mode[1]	8.55	8.71	9.43	11.64	7.64	8.43	9.48	11.44	8.93	10.52	11.62	14.16	16.58	19.03	22.48	27.42	5.84	5.9
General Instability	(2)*	(2)	(2)	(2)	(2)	(2)	(2)	(2)	(2)	(2)	(2)	(3)	(2)	(2)	(3)	(3)	(2)	(2
drick Part III[9]	5.79	3.93	2.68	1.78	4.87	3.82	2.89	2.26	4.45	4.05	3.52	2.61	5.12	5.23	4.22	3.04	3.53	2.7
dified Bryant[3]	6.70	4.38	2.86	1.81	5.32	4.13	3.07	2.29	4.73	4.28	3.62	2.54	5.12	5.09	4.27	2.79	4.09	3.0
tic Shell Buckling																		
symmetric Mode[7]	1.06	1.03	1.06	1.23	1.07	1.15	> 1.2	> 1.3	1.09	> 1.1	> 1.2	> 1.3	> 1.1	> 1.1	> 1.1	> 1.1	1.11	1.0
c Mode (Lunchick)[1]	1.04	1.05	1.13	1.35	1.00	1.08	> 1.2	> 1.3	1.06	> 1.1	> 1.2	> 1.3	> 1.1	> 1.1	> 1.1	> 1.1	1.11	1.1
: General Instability R_t^3	1.17	1.06	1.02	1.05	0.98	1.03	1.04	1.08	0.96	1.03	1.03	1.07	0.93	1.02	1.04	1.07	1.27	1.1
Lunchick[2]	1.18	1.07	1.04	1.08	1.00	1.06	1.08	1.15	1.00	1.09	1.10	1.08	0.99	1.06	1.06	1.11	1.30	1.2
$\frac{\sigma_{yh}}{R_o}\left(1+\frac{A_f}{ht_f}\right)$	1.13	0.99	0.95	1.00	0.92	0.97	0.97	1.01	0.93	0.97	0.95	0.99	0.90	0.92	0.95	0.99	1.25	1.1
p_{st}^3	1.17	1.06	1.04	1.07	0.99	1.04	1.06	1.11	0.98	1.05	1.06	1.07	0.96	1.03	1.05	1.09	1.29	1.
ed Mode of Collapse	I**	I	III	III	I	III	III	III	III	III	III	III	III	III	III	III	I	I

etical number of circumferential lobes in parentheses.

Inelastic shell buckling (axisymmetric)
Inelastic shell buckling (nonsymmetric)
Inelastic General Instability
Elastic General Instability

al to Adjusted Experimental Collapse Pressure																			
0-82	25-58	25-56	25-54	25-52	20-58	20-56	20-54	20-52	15-58	15-56	15-54	15-52	10-58	10-56	10-54	10-52	25-28	25-26	25-24
1.54	0.68	0.73	0.84	1.25	0.72	0.77	1.06	1.38	0.76	0.90	1.13	1.51	0.91	1.05	1.27	1.62	0.75	0.83	0.98
0.93	0.85	0.82	0.81	0.97	0.82	0.79	0.87	0.99	0.78	0.82	0.90	0.99	0.80	0.85	0.91	0.99	1.01	0.97	1.01
1.08	1.04	1.01	0.98	1.15	0.99	0.95	1.03	1.16	0.90	0.96	1.05	1.15	0.91	0.97	1.05	1.15	1.23	1.17	1.22
1.07	0.86	0.87	0.89	1.09	0.84	0.83	0.96	1.12	0.82	0.89	1.0[illegible]	1.13	0.87	0.94	1.03	1.14	0.96	0.96	1.05
1.08	0.98	0.96	0.95	1.13	0.93	0.90	1.01	1.15	0.87	0.93	1.04	1.14	0.89	0.96	1.04	1.15	1.13	1.09	1.16
23.18	3.61	3.47	3.53	4.21	4.43	4.32	4.68	5.50	5.46	6.07	6.96	7.97	9.29	10.39	12.55	15.38	1.79	1.71	1.69
27.42	5.84	5.90	6.01	7.53	5.19	5.24	5.94	7.26	5.60	6.53	7.67	9.26	11.14	12.50	14.99	17.91	2.86	2.78	2.87
(3)	(2)	(2)	(2)	(3)	(2)	(2)	(3)	(3)	(2)	(3)	(3)	(3)	(3)	(3)	(3)	(4)	(3)	(3)	(3)
3.04	3.53	2.72	2.06	1.57	3.57	2.91	2.78	1.37	3.96	3.66	2.64	1.81	4.14	3.60	3.08	2.21	2.49	1.85	1.23
2.79	4.09	3.04	2.22	1.62	3.94	3.12	3.03	1.59	4.08	4.00	2.80	1.79	4.44	3.74	3.02	2.10	3.21	2.17	1.54
1.1	1.11	1.07	1.05	1.23	1.11	1.07	1.17	1.31	1.08	1.15	1.28	1.40	> 1.1	> 1.1	> 1.2	> 1.3	1.14	1.13	1.16
1.1	1.11	1.11	1.08	1.29	1.05	1.06	1.19	1.37	1.00	1.06	1.26	1.39	> 1.1	> 1.1	> 1.2	> 1.3	1.27	1.17	1.21
1.07	1.27	1.16	1.06	1.12	1.13	1.05	1.10	1.11	1.01	1.05	1.09	1.11	1.00	1.03	1.06	1.11	1.43	1.29	1.24
1.11	1.30	1.20	1.11	1.13	1.18	1.10	1.10	1.13	1.07	1.06	1.10	1.14	1.02	1.08	1.12	1.13	1.45	1.32	1.26
0.99	1.25	1.12	1.01	1.08	1.12	1.01	1.02	1.07	0.99	0.99	1.02	1.06	0.98	0.98	1.01	1.05	1.49	1.29	1.24
1.09	1.29	1.18	1.08	1.12	1.15	1.06	1.12	1.12	1.03	1.05	1.09	1.12	1.01	1.05	1.10	1.12	1.44	1.30	1.25
III	I	I	III	III	I	I	III	III	III	III	III	III	III	III	III	III	I	I	III

TABLE 6 (Continued)

Model	Ratio of Theoretical to Adjusted E																	
	20-28	20-26	20-24	15-28	15-26	15-24	10-28	10-26	10-24	10-22	15-58F	15-56F	15-54F	15-52F	10-58F	10-56F	10-54F	10-52F
ı Stress Criterion																		
tudinal, Frame	0.82	0.93	1.12	0.91	1.01	1.25	1.05	1.19	1.42	1.86	0.75	0.86	1.09	1.41	0.87	1.03	1.19	1.52
erential, Midbay	1.01	1.00	1.00	0.99	0.96	1.01	0.95	0.98	1.04	1.17	0.74	0.76	0.82	0.90	0.74	0.80	0.86	0.91
ky-Von Mises																		
ss Criterion																		
ay, Midplane	1.21	1.20	1.18	1.15	1.12	1.18	1.07	1.12	1.20	1.36	0.85	0.89	0.95	1.05	0.83	0.91	0.98	1.0
bay, Outside	0.99	1.05	1.09	1.02	1.03	1.13	1.02	1.08	1.17	1.34	0.79	0.83	0.92	1.03	0.81	0.89	0.97	1.0
k Plastic Hinge[4]	1.13	1.16	1.15	1.10	1.09	1.17	1.05	1.10	1.19	1.35	0.83	0.87	0.94	1.04	0.83	0.90	0.98	1.0
c Shell Buckling																		
mmetric Mode[7]	2.09	2.13	2.20	2.69	2.77	3.09	4.50	5.03	5.35	7.29	5.29	5.71	6.41	7.42	8.69	9.97	11.53	14.1
metric Mode[1]	2.41	2.52	2.78	2.76	2.93	3.40	5.25	5.86	6.32	7.89	5.64	6.24	7.27	8.72	10.47	11.96	13.76	16.6
General Instability	(3)	(3)	(4)	(4)	(4)	(4)	(4)	(4)	(5)	(6)	(2)	(3)	(3)	(3)	(3)	(3)	(3)	(4
trick Part III[9]	2.38	2.02	1.39	2.70	1.89	1.48	2.44	2.17	1.70	1.27	3.76	3.39	2.32	1.61	3.83	3.39	3.37	1.6
lified Bryant[3]	2.75	2.19	1.55	2.78	2.03	1.57	2.48	2.16	1.79	1.26	3.88	3.73	2.47	1.61	4.10	3.52	3.43	1.5
ic Shell Buckling																		
ymmetric Mode[7]	1.20	1.19	1.20	1.23	1.20	1.26	> 1.2	> 1.3	> 1.4	> 1.6	1.02	1.04	1.12	1.25	> 1.1	> 1.1	> 1.2	> 1.2
c Mode (Lunchick)[1]	1.20	1.20	1.20	1.19	1.16	1.24	> 1.2	> 1.3	> 1.4	> 1.6	0.99	1.02	1.14	1.26	> 1.1	> 1.1	> 1.2	> 1.2
General Instability																		
ρ_t^3	1.31	1.25	1.17	1.20	1.13	1.16	1.12	1.14	1.16	1.24	0.96	0.97	0.97	0.97	0.93	0.98	1.01	0.
Lunchick[2]	1.33	1.28	1.18	1.23	1.15	1.17	1.16	1.16	1.17	1.24	1.02	0.99	1.00	1.01	0.96	1.01	1.07	0.
$\frac{\sigma_{yh}}{R_o}\left(1+\frac{A_f}{hL_f}\right)$	1.33	1.24	1.15	1.23	1.12	1.13	1.12	1.14	1.13	1.23	0.92	0.91	0.91	0.95	0.89	0.92	0.96	0.
ρ_{st}^3	1.31	1.26	1.17	1.23	1.14	1.16	1.12	1.15	1.17	1.24	0.99	0.98	0.98	0.99	0.94	0.99	1.04	0
l Mode of Collapse	I	I	III	I	III	III	III	III	III	III	I	III	III	III	III	III	III	II

etical number of circumferential lobes in parentheses.

nelastic shell buckling (axisymmetric)
inelastic shell buckling (nonsymmetric)
Inelastic General Instability
Elastic General Instability

mental Collapse Pressure															
28F	25-26F	25-24F	25-22F	20-28F	20-26F	20-24F	20-22F	15-28F	15-26F	15-24F	15-22F	10-28F	10-26F	10-24F	10-22F
80	0.93	0.99		0.84	0.91	1.05		0.92	1.03	1.24		1.05	1.13	1.33	1.70
98	0.96	0.96		0.98	0.94	0.93		0.91	0.91	0.95		0.90	0.92	0.95	1.06
19	1.12	1.16		1.17	1.12	1.10		1.05	1.05	1.11		1.01	1.04	1.09	1.23
96	1.00	1.03		0.98	0.98	1.02		0.96	0.99	1.07		0.98	1.02	1.07	1.22
10	1.10	1.11		1.09	1.07	1.07		1.02	1.03	1.10		1.00	1.03	1.08	1.23
50	1.50	1.59	2.07	2.08	2.05	1.95	2.61	2.49	2.62	2.80	3.45	3.85	4.32	5.11	6.35
48	2.59	2.79	3.82	2.48	2.53	2.58	3.52	2.64	2.85	3.15	4.01	4.64	5.20	6.09	7.50
(3)	(3)	(3)	(4)	(3)	(3)	(4)	(4)	(4)	(4)	(4)	(5)	(4)	(4)	(5)	(6)
15	1.65	1.31	0.85	2.34	1.92	1.35	0.91	2.50	1.47	1.40	0.97	2.29	2.07	1.57	1.17
57	1.90	1.46	0.93	2.70	2.11	1.55	0.98	2.61	2.02	1.51	1.06	2.39	2.08	1.69	1.23
14	1.12	1.10		1.18	1.14	1.15		1.18	1.19	1.27		>1.2	>1.3	>1.4	>1.4
19	1.19	1.19		1.17	1.15	1.18		1.16	1.16	1.28		>1.2	>1.3	>1.4	>1.4
31	1.19	1.12		1.24	1.14	0.98		1.08	1.04	1.03		1.03	1.03	1.02	1.07
34	1.21	1.15		1.28	1.18	1.06		1.11	1.06	1.06		1.06	1.07	1.02	1.07
35	1.20	1.16		1.29	1.16	1.07		1.11	1.05	1.05		1.04	1.05	1.03	1.12
33	1.20	1.14		1.26	1.16	1.05		1.11	1.05	1.04		1.04	1.06	1.02	1.07
	I	II	III-e	I	I	III	III-e	I	III	III	III-e	III	III	III	III

REFERENCES

1. Lunchick, M.E., "Plastic Axisymmetric Buckling of Ring-Stiffened Cylindrical Shells Fabricated from Strain-Hardening Materials and Subjected to External Hydrostatic Pressure," David Taylor Model Basin Report 1393 (Jan 1961).

2. Lunchick, M.E., "Plastic General Instability of Ring-Stiffened Cylindrical Shells," David Taylor Model Basin Report 1587 (Sep 1963).

3. Krenzke, M.A. and Kiernan, T.J., "Structural Development of a Titanium Oceanographic Vehicle for Operating Depths of 15,000 to 20,000 Feet," David Taylor Model Basin Report 1677 (Sep 1963).

4. Lunchick, M.E., "Yield Failure of Stiffened Cylinders under Hydrostatic Pressure," Proceedings Third U. S. National Congress of Applied Mechanics (Jun 1958). Also David Taylor Model Basin Report 1291 (Jan 1959).

5. Pulos, J.G. and Salerno, V.L., "Axisymmetric Elastic Deformations and Stresses in a Ring-Stiffened, Perfectly Circular Cylindrical Shell under Hydrostatic Pressure," David Taylor Model Basin Report 1497 (Sep 1961).

6. Short, R.D., "Effective Area of Ring Stiffeners for Axially Symmetric Shells," David Taylor Model Basin Report 1894 (Mar 1964).

7. Reynolds, T.E., "Inelastic Lobar Buckling of Cylindrical Shells under External Hydrostatic Pressure," David Taylor Model Basin Report 1392 (Aug 1960).

8. Krenzke, M.A., et al., "Potential Hull Structures for Rescue and Search Vehicles of the Deep Submergence Systems Project," David Taylor Model Basin Report 1985 (Mar 1965).

9. Kendrick, S., "The Buckling under External Pressure of Circular Cylindrical Shells with Evenly Spaced Equal Strength Circular Ring Frames – Part III," Naval Construction Research Establishment Report R244 (Sep 1953).

INITIAL DISTRIBUTION

Copies	
16	CHBUSHIPS
	2 Sci & Res Sec (Code 442)
	1 Lab Mgt (Code 320)
	3 Tech Info Br (Code 210L)
	1 Struc Mech, Hull Mat & Fab (Code 341A)
	1 Prelim Des Br (Code 420)
	2 Prelim Des Sec (Code 421)
	1 Ship Protec (Code 423)
	1 Hull Des Br (Code 440)
	1 Struc Sec (Code 443)
	1 Sub Br (Code 525)
	1 Hull Arrgt, Struc, & Preserv (Code 633)
	1 Pres Ves Sec (Code 651F)
2	CHONR
	1 Struc Mech Br (Code 439)
	1 Undersea Programs (Code 466)
4	CNO
	1 Tech Anal & Adv Gr (Op 07T)
	1 Plans, Programs & Req Br (Op 311)
	1 Sub Program Br (Op 713)
	1 Tech Support Br (Op 725)
2	CHBUWEPS, SP-001
10	CDR, DDC
1	CO & DIR, USNMEL
1	CDR, USNOL
1	DIR, USNRL (Code 2027)
1	CO & DIR, USNUSL
1	CO & DIR, USNEL
1	CDR, USNOTS, China Lake
1	CDR, USNOTS, Pasadena
1	CO, USNUOS
2	NAVSHIPYD PTSMH
2	NAVSHIPYD MARE
1	NAVSHIPYD CHASN
1	SUPSHIP, Groton
1	EB Div, Gen Dyn Corp

Copies	
1	SUPSHIP, Newport News
1	NNSB & DD Co
1	SUPSHIP, Pascagoula
1	Ingalls Shipbldg Corp
1	SUPSHIP, Camden
1	New York Shipbldg Corp
1	DIR, DEF R&E, Attn: Tech Lib
1	CO, USNROTC & NAVADMINU, MIT
1	O in C, PGSCOL, Webb
1	DIR, APL, Univ of Washington, Seattle
1	NAS, Attn: Comm on Undersea Warfare
1	WHOI
	1 Mr. J. Mavor
1	Dr. E. Wenk, Jr., Library of Congress
1	Dr. R. DeHart, SWRI
1	Mr. L.P. Zick, Chic Bridge & Iron Co, Chicago
1	Prof. E.O. Waters, Yale University
2	Mr. C.F. Larson, Sec, Welding Res Council
1	Mr. J.L. Mershon, AEC

UNCLASSIFIED

Security Classification

DOCUMENT CONTROL DATA - R&D

(Security classification of title, body of abstract and indexing annotation must be entered when the overall report is classified)

1 ORIGINATING ACTIVITY (Corporate author) David Taylor Model Basin	2a. REPORT SECURITY CLASSIFICATION UNCLASSIFIED 2b. GROUP

3 REPORT TITLE

INELASTIC BUCKLING TESTS OF RING-STIFFENED CYLINDERS UNDER HYDROSTATIC PRESSURE

4. DESCRIPTIVE NOTES (Type of report and inclusive dates)

Final Report

5. AUTHOR(S) (Last name, first name, initial)

Boichot, Lance and Reynolds, Thomas E.

6. REPORT DATE	7a. TOTAL NO. OF PAGES	7b. NO. OF REFS
May 1965	33	9

8a. CONTRACT OR GRANT NO. b. PROJECT NO. S-F013 03 02 c. Task 1951 d.	9a. ORIGINATOR'S REPORT NUMBER(S) 1992 9b. OTHER REPORT NO(S) (Any other numbers that may be assigned this report)

10. AVAILABILITY/LIMITATION NOTICES

11. SUPPLEMENTARY NOTES	12. SPONSORING MILITARY ACTIVITY Bureau of Ships

13 ABSTRACT

A series of small machined aluminum models were collapsed under external hydrostatic pressure to study the inelastic buckling of near-perfect ring-stiffened cylinders made of strain-hardening materials. The predominant modes of failure were general instability and axisymmetric shell buckling.

Comparisons of test results with the analyses of Lunchick, Krenzke, and Kiernan show promising correlation but additional data would be needed for a complete evaluation.

High bending stresses near frames did not noticeably affect axisymmetric shell buckling strength. The presence of frame fillets, however, caused a significant increase in general instability strength although bending stresses in the absence of fillets were relatively low.

DD FORM 1 JAN 64 1473

(ENCLOSURE 1)

UNCLASSIFIED

Security Classification

14. KEY WORDS	LINK A		LINK B		LINK C	
	ROLE	WT	ROLE	WT	ROLE	WT
Ring-Stiffened Cylinders						
Hydrostatic Pressure						
Buckling						
Inelastic Buckling						
General Instability						

INSTRUCTIONS

1. ORIGINATING ACTIVITY: Enter the name and address of the contractor, subcontractor, grantee, Department of Defense activity or other organization *(corporate author)* issuing the report.

2a. REPORT SECURITY CLASSIFICATION. Enter the overall security classification of the report. Indicate whether "Restricted Data" is included. Marking is to be in accordance with appropriate security regulations.

2b. GROUP: Automatic downgrading is specified in DoD Directive 5200.10 and Armed Forces Industrial Manual. Enter the group number. Also, when applicable, show that optional markings have been used for Group 3 and Group 4 as authorized.

3. REPORT TITLE: Enter the complete report title in all capital letters. Titles in all cases should be unclassified. If a meaningful title cannot be selected without classification, show title classification in all capitals in parenthesis immediately following the title.

4. DESCRIPTIVE NOTES: If appropriate, enter the type of report, e.g., interim, progress, summary, annual, or final. Give the inclusive dates when a specific reporting period is covered.

5. AUTHOR(S): Enter the name(s) of author(s) as shown on or in the report. Enter last name, first name, middle initial. If military, show rank and branch of service. The name of the principal author is an absolute minimum requirement.

6. REPORT DATE: Enter the date of the report as day, month, year; or month, year. If more than one date appears on the report, use date of publication.

7a. TOTAL NUMBER OF PAGES: The total page count should follow normal pagination procedures, i.e., enter the number of pages containing information.

7b. NUMBER OF REFERENCES: Enter the total number of references cited in the report.

8a. CONTRACT OR GRANT NUMBER: If appropriate, enter the applicable number of the contract or grant under which the report was written.

8b, 8c, & 8d. PROJECT NUMBER: Enter the appropriate military department identification, such as project number, subproject number, system numbers, task number, etc.

9a. ORIGINATOR'S REPORT NUMBER(S): Enter the official report number by which the document will be identified and controlled by the originating activity. This number must be unique to this report.

9b. OTHER REPORT NUMBER(S): If the report has been assigned any other report numbers *(either by the originator or by the sponsor)*, also enter this number(s).

10. AVAILABILITY/LIMITATION NOTICES: Enter any limitations on further dissemination of the report, other than those imposed by security classification, using standard statements such as:

(1) "Qualified requesters may obtain copies of this report from DDC."

(2) "Foreign announcement and dissemination of this report by DDC is not authorized."

(3) "U. S. Government agencies may obtain copies of this report directly from DDC. Other qualified DDC users shall request through _____."

(4) "U. S. military agencies may obtain copies of this report directly from DDC. Other qualified users shall request through _____."

(5) "All distribution of this report is controlled. Qualified DDC users shall request through _____."

If the report has been furnished to the Office of Technical Services, Department of Commerce, for sale to the public, indicate this fact and enter the price, if known.

11. SUPPLEMENTARY NOTES: Use for additional explanatory notes.

12. SPONSORING MILITARY ACTIVITY: Enter the name of the departmental project office or laboratory sponsoring *(paying for)* the research and development. Include address.

13. ABSTRACT: Enter an abstract giving a brief and factual summary of the document indicative of the report, even though it may also appear elsewhere in the body of the technical report. If additional space is required, a continuation sheet shall be attached.

It is highly desirable that the abstract of classified reports be unclassified. Each paragraph of the abstract shall end with an indication of the military security classification of the information in the paragraph, represented as *(TS), (S), (C), or (U)*.

There is no limitation on the length of the abstract. However, the suggested length is from 150 to 225 words.

14. KEY WORDS: Key words are technically meaningful terms or short phrases that characterize a report and may be used as index entries for cataloging the report. Key words must be selected so that no security classification is required. Identifiers, such as equipment model designation, trade name, military project code name, geographic location, may be used as key words but will be followed by an indication of technical context. The assignment of links, roles, and weights is optional.

David Taylor Model Basin. Report 1992.
INELASTIC BUCKLING TESTS OF RING-STIFFENED CYLINDERS UNDER HYDROSTATIC PRESSURE, by Lance Boichot and Thomas E. Reynolds. May 1965. iii, 33p. illus., diagrs., graphs, tables, refs. UNCLASSIFIED

A series of small machined aluminum models were collapsed under external hydrostatic pressure to study the inelastic buckling of near-perfect ring-stiffened cylinders made of strain-hardening materials. The predominant modes of failure were general instability and axisymmetric shell buckling.

Comparisons of test results with the analyses of Lunchick, Krenzke, and Kiernan show promising correlation but additional data would be needed for a complete evaluation.

High bending stresses near frames did not noticeably affect axisymmetric shell buckling strength. The presence of frame

1. Cylindrical shells (Stiffened)--Hydrostatic pressure--Measurement
2. Cylindrical shells (Stiffened)--Collapse--Model tests
3. Cylindrical shells (Stiffened)--Buckling--Model tests

I. Boichot, Lance
II. Reynolds, Thomas E.
III. S-F013 03 02, Task 1951.

David Taylor Model Basin. Report 1992.
INELASTIC BUCKLING TESTS OF RING-STIFFENED CYLINDERS UNDER HYDROSTATIC PRESSURE, by Lance Boichot and Thomas E. Reynolds. May 1965. iii, 33p. illus., diagrs., graphs, tables, refs. UNCLASSIFIED

A series of small machined aluminum models were collapsed under external hydrostatic pressure to study the inelastic buckling of near-perfect ring-stiffened cylinders made of strain-hardening materials. The predominant modes of failure were general instability and axisymmetric shell buckling.

Comparisons of test results with the analyses of Lunchick, Krenzke, and Kiernan show promising correlation but additional data would be needed for a complete evaluation.

High bending stresses near frames did not noticeably affect axisymmetric shell buckling strength. The presence of frame

1. Cylindrical shells (Stiffened)--Hydrostatic pressure--Measurement
2. Cylindrical shells (Stiffened)--Collapse--Model tests
3. Cylindrical shells (Stiffened)--Buckling--Model tests

I. Boichot, Lance
II Reynolds, Thomas E.
III. S-F013 03 02, Task 1951.

David Taylor Model Basin. Report 1992.
INELASTIC BUCKLING TESTS OF RING-STIFFENED CYLINDERS UNDER HYDROSTATIC PRESSURE, by Lance Boichot and Thomas E. Reynolds. May 1965. iii, 33p. illus., diagrs., graphs, tables, refs. UNCLASSIFIED

A series of small machined aluminum models were collapsed under external hydrostatic pressure to study the inelastic buckling of near-perfect ring-stiffened cylinders made of strain-hardening materials. The predominant modes of failure were general instability and axisymmetric shell buckling.

Comparisons of test results with the analyses of Lunchick, Krenzke, and Kiernan show promising correlation but additional data would be needed for a complete evaluation.

High bending stresses near frames did not noticeably affect axisymmetric shell buckling strength. The presence of frame

1. Cylindrical shells (Stiffened)--Hydrostatic pressure--Measurement
2. Cylindrical shells (Stiffened)--Collapse--Model tests
3. Cylindrical shells (Stiffened)--Buckling--Model tests

I. Boichot, Lance
II. Reynolds, Thomas E.
III. S-F013 03 02, Task 1951.

David Taylor Model Basin. Report 1992.
INELASTIC BUCKLING TESTS OF RING-STIFFENED CYLINDERS UNDER HYDROSTATIC PRESSURE, by Lance Boichot and Thomas E. Reynolds. May 1965. iii, 33p. illus., diagrs., graphs, tables, refs. UNCLASSIFIED

A series of small machined aluminum models were collapsed under external hydrostatic pressure to study the inelastic buckling of near-perfect ring-stiffened cylinders made of strain-hardening materials. The predominant modes of failure were general instability and axisymmetric shell buckling.

Comparisons of test results with the analyses of Lunchick, Krenzke, and Kiernan show promising correlation but additional data would be needed for a complete evaluation.

High bending stresses near frames did not noticeably affect axisymmetric shell buckling strength. The presence of frame

1. Cylindrical shells (Stiffened)--Hydrostatic pressure--Measurement
2. Cylindrical shells (Stiffened)--Collapse--Model tests
3. Cylindrical shells (Stiffened)--Buckling--Model tests

I. Boichot, Lance
II. Reynolds, Thomas E.
III. S-F013 03 02, Task 1951.

fillets, however, caused a significant increase in general instability strength although bending stresses in the absence of fillets were relatively low.

fillets, however, caused a significant increase in general instability strength although bending stresses in the absence of fillets were relatively low.

fillets, however, caused a significant increase in general instability strength although bending stresses in the absence of fillets were relatively low.

fillets, however, caused a significant increase in general instability strength although bending stresses in the absence of fillets were relatively low.